Ⅳ．研究成果の刊行物・別冊

Journal of Clinical Microbiology

Molecular Epidemiologic Analysis and Antimicrobial Resistance of Helicobacter cinaedi Isolated from Seven Hospitals in Japan

Emiko Rimbara, Shigetarou Mori, Mari Matsui, Satowa Suzuki, Jun-ichi Wachino, Yoshiaki Kawamura, Zeli Shen, James G. Fox and Keigo Shibayama

J. Clin. Microbiol. **2012, 50(8):2553. DOI: 10.1128/JCM.06810-11.**
Published Ahead of Print 16 May 2012.

JCM
Journals.ASM.org

Molecular Epidemiologic Analysis and Antimicrobial Resistance of *Helicobacter cinaedi* Isolated from Seven Hospitals in Japan

Emiko Rimbara,[a] Shigetarou Mori,[a] Mari Matsui,[a] Satowa Suzuki,[a] Jun-ichi Wachino,[a] Yoshiaki Kawamura,[b] Zeli Shen,[c] James G. Fox,[c] and Keigo Shibayama[a]

Department of Bacteriology II, National Institute of Infectious Diseases, Tokyo, Japan[a]; Department of Microbiology, School of Pharmacy, Aichi Gakuin University, Aichi, Japan[b]; and Division of Comparative Medicine, Massachusetts Institute of Technology, Cambridge, Massachusetts, USA[c]

Helicobacter cinaedi **colonizes the colons of human and animals and can cause colitis, cellulitis, and sepsis in humans, with infections in immunocompromised patients being increasingly recognized. However, methods for analyzing the molecular epidemiology of *H. cinaedi* are not yet established. A genotyping method involving multilocus sequence typing (MLST) was developed and used to analyze 50 *H. cinaedi* isolates from Japanese hospitals in addition to 6 reference strains. Pulsed-field gel electrophoresis (PFGE) results were also compared with the MLST results. Based on the genomic information from strain CCUG18818, 21 housekeeping genes were selected as candidates for MLST and were observed to have high homology (96.5 to 100%) between isolates. Following a comparison of the 21 housekeeping genes from 8 *H. cinaedi* isolates, 7 genes were chosen for MLST, revealing 14 sequence types (STs). The isolates from 3 hospitals belonged to the same STs, but the isolates from the other 4 hospitals belonged to different STs. Isolates belonging to ST6 were analyzed by PFGE and showed similar, but not identical, patterns between isolates. Isolates belonging to ST9, ST10, and ST11, which belonged to the same clonal complex, had the same pattern. All isolates were found to contain mutations in GyrA and the 23S rRNA gene that confer ciprofloxacin and clarithromycin resistance, respectively, in *H. cinaedi*. These results raise concerns about the increase in *H. cinaedi* isolates resistant to clarithromycin and ciprofloxacin in Japan.**

Helicobacter cinaedi is a motile, Gram-negative, spiral bacterium that colonizes the colons of humans and animals; it is mainly isolated from blood and feces. The first *H. cinaedi* infection in humans was reported in 1984, after isolation from a homosexual man (32). Since then, *H. cinaedi* infections have usually been detected in immunocompromised patients (1, 12, 13, 15, 16, 20, 31), although in some cases, they may also occur in patients with normal immunity (9, 33). The clinical manifestations of *H. cinaedi* include enteritis, proctocolitis, cellulitis, arthritis, and bacteremia. Septicemia and meningitis resulting from an *H. cinaedi* infection have also been observed in a neonate (21).

The prevalence of *H. cinaedi* in humans and other animals has not been well investigated, and the mechanism and timing of *H. cinaedi* infection remain controversial. Since *H. cinaedi* has been detected in the feces of normal animals, including hamsters and monkeys, these animals may be natural reservoirs for *H. cinaedi* (5, 7). However, as the growth of *H. cinaedi* is slower than that of other bacteria present in the colon, the presence of *H. cinaedi* in feces may be undetected in some cases. In addition, the atmospheric conditions required for the growth of *H. cinaedi* are not commonly available in most laboratories. Indeed, the number of reports of *H. cinaedi* infection have increased as the knowledge of *Helicobacter* spp. has expanded, and the possible nosocomial spread of *H. cinaedi* was recently reported (18).

To identify the routes of *H. cinaedi* transmission, molecular epidemiologic analyses are required; however, a method is not yet available to classify *H. cinaedi* isolates. Many molecular epidemiologic tools, such as pulsed-field gel electrophoresis (PFGE), ribotyping, restriction fragment length polymorphism, and arbitrary-primer PCR, have been developed for use in bacteria. However, multilocus sequence typing (MLST) is increasingly becoming one of the gold standards by which isolates can be classified and identified as a result of the progressive improvements in DNA sequencing techniques (4, 25). PFGE is a highly discriminatory typing method that has been used for epidemiological analysis of many pathogenic bacteria. However, it is difficult to obtain clear band patterns using PFGE in some cases, and a low typeability of *H. pylori* by this technique has been reported (2). In contrast, the genomic DNA sequences needed for MLST analysis can be obtained from any isolate, if the appropriate culture conditions are available. MLST can also be used to analyze the genetic interrelationship between isolates. Therefore, MLST would be useful for elucidating the route of *H. cinaedi* infection. In this study, we developed MLST for *H. cinaedi* and compared the results obtained with observed PFGE patterns. Since the antimicrobial susceptibilities of *H. cinaedi* isolates from Japan have not yet been reported, we also measured antimicrobial susceptibilities and analyzed the genes related to antimicrobial resistance.

MATERIALS AND METHODS

H. cinaedi **isolates and culture.** Fifty *H. cinaedi* isolates were obtained from blood or fecal samples from patients treated in seven hospitals in Japan. Twelve isolates were obtained from Sapporo City General Hospital (hospital A) in Sapporo; the other 38 isolates were obtained from six hospitals in Tokyo: 2 isolates from the Social Insurance Chuo General Hospital (hospital B), 6 isolates from Toranomon Hospital (hospital C), 6 isolates from Teikyo University Hospital (hospital D), 3 isolates from

Received 10 January 2012 Returned for modification 21 February 2012
Accepted 28 April 2012
Published ahead of print 16 May 2012
Address correspondence to Emiko Rimbara, rimbara@nih.go.jp.
Supplemental material for this article may be found at http://jcm.asm.org/.

doi:10.1128/JCM.06810-11

TABLE 1 Genes and primers used for MLST analysis of *H. cinaedi*

Gene	ID	Putative gene product	Primer (5′–3′)		Product size (bp)
			Forward	Reverse	
23S rRNA	AY596254	23S rRNA	GAAGGACGTACTAAGCTGCGAT	GTTTGGCCTTTCACCCCTAT	762
ppa	HCCG_01345	Inorganic pyrophosphatase	TCTCTCAAAAGTATCAGTAGGCGA	GCCCTTGTAGGCTTTGATTG	514
aspA	HCCG_00537	Aspartate ammonia-lyase	GGCGGCTCTAGCAAATAATG	CCGTATCTTGTGTCGCTTCA	650
aroE	HCCG_00648	Shikimate 5-dehydrogenase	CGCACATTCTAAATCCCCAC	TAAGGCTAGGGCTGCTTGAT	688
atpA	HCCG_02167	ATP synthase subunit alpha	TGTGGTTGGACGCGTTATTA	TGGCAATGCTGTAAGTGAGC	646
tkt	HCCG_01495	Transketolase	AATCTGCTTCACTAGCCGGA	CTGTGGAAAATCGCCTTCAT	665
cdtB	HCCG_01069	Cytolethal distending toxin B subunit	GGTGTAGCATTTGGTGCGAT	TCAAGTATGCCTCCGCTTCT	635

Nihon University Itabashi Hospital (hospital E), 4 isolates from Toho University (hospital F), and 17 isolates from Surugadai Nihon University Hospital (hospital G). Details regarding the clinical manifestation of the patients were available only for the 26 isolates from hospitals A to D. These patients consisted of 7 women and 19 men, with a mean age of 61.3 years (age range, 28 to 88 years). Most of these patients were immunocompromised and had diseases such as malignant lymphoma, non-Hodgkin's lymphoma, and chronic renal failure. Four of the 26 isolates were obtained from feces, 1 was from a colon biopsy specimen, and the remaining isolates were recovered from patient blood samples. The 12 isolates from hospital A were isolated from the same ward between April and June 2008. Two isolates from hospital B were also isolated from the same ward in May 2005. Of the 6 isolates from hospital C, 2 were from same ward in October 2004, and the remaining 4 isolates were isolated sporadically from different wards in 2000 and 2008. Six isolates from hospital D were isolated sporadically between 2003 and 2008. The 6 reference strains used in this study—CCUG18818, CCUG18819, CCUG43521, MIT 99-5915, MIT 00-5434, and MIT 01-5002—were previously described by Taylor et al. (30). CCUG18818, CCUG18819, and MIT 99-5915 were human isolates from the United States recovered in 1986, 1986, and 1999, respectively. CCUG43521 was isolated from a human in Australia in 2000. MIT 00-5434 and MIT 00-5002 were isolated from rhesus monkeys in the United States in 1999 and 2000, respectively.

All isolates were subcultured on brucella agar (Becton, Dickinson, Franklin Lakes, NJ), with 5% horse blood, under microaerobic conditions with hydrogen obtained by the gas replacement method using an anaerobic gas mixture (H_2, 10%; CO_2, 10%; and N_2, 80%) (5, 6). *H. cinaedi* isolates were identified by morphological analysis and by DNA sequencing of both the 16S rRNA and the 23S rRNA genes. The primers H276f (5′-CTATGACGGGTATCCGGC-3′) and C05R (5′-ACTTCACCCCAG TCGCTG-3′), reported by Riley et al. (22), were used for amplification and DNA sequencing of the 16S rRNA gene. For the amplification and DNA sequencing of the 23S rRNA gene, the same primers used for MLST (described below) were used.

Multilocus sequence typing. Genomic information for CCUG18818 was obtained from the NCBI database (http://www.ncbi.nlm.nih.gov/sites/genome), and 21 genes, chosen mainly from genes used for MLST of *H. pylori* and *Campylobacter* spp., were selected as candidate genes for MLST (see Table S1 in the supplemental material). *H. cinaedi* genomic DNA was obtained by the classical phenol-chloroform DNA extraction method, as described by Stauffer et al. (26). Primers for each gene were designed using Primer3 software (http://frodo.wi.mit.edu/primer3/) to amplify approximately 700 bp of each gene. Amplification was performed using Ex Taq polymerase (TaKaRa Bio Inc., Shiga, Japan) under the following conditions: initial denaturation at 94°C for 2 min, followed by 35 cycles of 94°C for 30 s, 58°C for 20 s, and 72°C for 30 s, and a final extension step at 72°C for 5 min. PCR products were analyzed by DNA sequencing using the same primers used for amplification. Eight isolates from 4 hospitals (2 from each hospital) were analyzed, and the sequences were compared to select the appropriate genes for MLST. Genes with high homology between isolates were excluded; the 7 genes listed in Table 1 were ultimately used for MLST analysis. Both strands of DNA from each isolate were sequenced, and each gene was analyzed in all the isolates to determine its allele number. Alignment was performed by ATGC version 6 software (Genetyx Corporation, Tokyo Japan). For each gene, the alleles of CCUG18818 were assigned allele number 1, and the alleles from number 2 onward were assigned for each gene, according to the order in which the genes were encountered. The sequence type (ST) was defined by the allelic profile determined based on the combination of the 7 alleles. A clonal complex (CC) was defined as a group of STs in which every ST shared 6 alleles with at least 1 other member of the group, using the eBURST software program (http://eburst.mlst.net/). The phylogeny for the 56 isolates was estimated using concatenated sequences, comprising the 7 loci, via the neighbor-joining method with the maximum composite likelihood model using MEGA (version 5.05) software (27).

Pulsed-field gel electrophoresis. The PFGE method for *Helicobacter hepaticus*, reported previously (24), was modified and used in this study. Organisms cultured for 3 days were harvested and suspended in a solution containing 1 M NaCl and 10 mM EDTA [pH 8.0] and then embedded in 1% low-melting-point agarose with plug molds (Bio-Rad, Hercules, CA). The plugs were treated with lysozyme (1 mg/ml) in a solution containing 1 M NaCl, 0.1 M EDTA [pH 8.0], 10 mM Tris-HCl, 0.2% sodium deoxycholate, and 0.5% sodium *N*-lauryl-sarcosine at 37°C for 4 h, followed by a 1-mg/ml solution of proteinase K in 0.25 M EDTA [pH 8.0], and 1% sodium *N*-lauryl-sarcosine at 50°C for 24 h. The plugs were washed four times with TE buffer (10 mM Tris-HCl and 1 mM EDTA [pH 8.0]). The DNA plugs were washed with a solution containing 10 mM Tris-HCl and 1 mM EDTA [pH 8.0] and then washed with restriction enzyme buffer (New England BioLabs, Ipswich, MA) before digestion. The plugs were digested with 10 U of XhoI (New England BioLabs) or 10 U of SpeI (New England BioLabs) per plug in fresh restriction enzyme buffer at 37°C overnight.

PFGE of the digested plugs was carried out by the CHEF Mapper system (Bio-Rad) using 1% PFGE-grade agarose in 0.5× TBE (45 mM Tris base, 45 mM boric acid, 1 mM EDTA [pH 8]) with the following autoalgorithm for XhoI-digested DNA: 20- to 600-kb range, 6 V/cm, 120° included angle, an initial switch time of 2.98 s, and a final switch time of 54.17 s, with a linear switch time ramp for 27 h at 14°C. For SpeI-digested DNA, an autoalgorithm with a 20- to 200-kb range, an initial switch time of 2.98 s, and a final switch time of 17.33 s was used. A lambda ladder (Bio-Rad) was used as the molecular mass standard. After electrophoresis, the gel was stained in ethidium bromide (0.5 μg/ml) for 1 h, and DNA bands were visualized under UV light. Unfortunately, due to the inability to reculture 32 of the 50 Japanese *H. cinaedi* isolates from the stocks stored at −80°C, PFGE could be performed for only 18 isolates, of which 11 were from hospital A, 3 were from hospital F, and 4 were from hospital G. The 6 reference strains were also analyzed by PFGE.

Antimicrobial susceptibilities. Since *H. cinaedi* causes bacteremia and sepsis, the susceptibilities of the isolates to antimicrobial agents used to treat systemic infections were measured using the agar dilution method. The susceptibilities of the previously mentioned 18 isolates from Japan and the 6 reference strains against the following antimicrobial agents were determined: amoxicillin-clavulanic acid, imipenem, clarithromycin, ciprofloxacin, minocycline, and gentamicin—drugs that

TABLE 2 Characteristics and allelic profiles of seven loci used for *H. cinaedi* MLST

Locus	Size (bp)	No (%) of polymorphic sites	Allelic profile[a] CC1 ST1	CC1 ST2	CC1 ST3	CC4 ST4	CC4 ST5	CC4 ST6	CC7 ST7	CC8 ST8	CC9 ST9	CC9 ST10	CC9 ST11	CC12 ST12	CC13 ST13	CC14 ST14
23S rRNA	658	4 (0.61)	1	1	1	3	3	3	4	3	3	4	2	5	3	3
ppa	411	13 (3.16)	1	1	1	3	3	2	2	4	2	2	2	5	4	4
aspA	532	6 (1.13)	1	1	1	3	3	3	5	4	2	2	2	2	2	2
aroE	572	21 (3.67)	1	1	1	1	1	1	4	3	2	2	2	5	4	6
atpA	536	5 (0.93)	1	1	1	2	4	2	3	2	2	2	2	5	2	2
tkt	562	3 (0.53)	1	4	4	2	2	2	4	3	1	1	1	1	4	1
cdtB	535	9 (1.68)	1	2	1	1	1	1	1	2	2	2	2	3	1	2

[a] ST, sequence type; CC, clonal complex.

might commonly be used to treat such infections. In brief, *H. cinaedi* cells were suspended in saline to achieve a turbidity equivalent to that of a McFarland 2.0 standard, and approximately 5 μl of the inoculum was spotted onto Muller Hinton agar (Becton, Dickinson) containing 5% horse blood and various concentrations of the antimicrobial agents. Concentrations of the antimicrobial agents ranged from 0.008 μg/ml to 128 μg/ml. The plates were incubated under microaerobic conditions for 2 days. The MIC was defined as the minimum concentration of the antimicrobial agent that inhibited the growth of *H. cinaedi*.

DNA sequencing of the 23S rRNA and *gyrA* genes of *H. cinaedi*. The 23S rRNA gene and the *gyrA* gene of *H. cinaedi* were amplified using primer pairs of 23S-F2 (5′-CGGTGCTCGAAGGTTAAGAG-3′) and 23S-R2 (5′-TTCAGCGGTTATCACATCCA-3′), and gyrA F (5′-TCTCA CACACGGAGCAAAAG-3′) and gyrA R (5′-CCTGCATTACCAAGGGC TAA-3′), respectively. These primers were also used for the DNA sequencing of the PCR products. The 23S rRNA sequences and GyrA amino acid sequences of all isolates were compared with those of CCUG18818 to identify mutations in the isolates used in this study.

RESULTS

Similarity of the 16S rRNA gene and the 23S rRNA gene between *H. cinaedi* isolates. A comparison of a 1,022-bp section of the 16S rRNA gene, corresponding to the region from position 329 to 1350 of the 16S rRNA gene of CCUG18818 (GenBank accession number AB275317) indicated that the 50 *H. cinaedi* isolates had 98.8 to 99.9% similarity with the CCUG18818 strain. A 658-bp region of the 23S rRNA gene, corresponding to the region from 75 to 732 of the 23S rRNA gene of CCUG18818 (GenBank accession number AY596254), was also compared among the 50 isolates and 6 reference strains; the results indicated 99.5 to 100% similarity, confirming that all the isolates used in this study were *H. cinaedi*.

Diversity of 21 housekeeping genes in *H. cinaedi*. To identify genes suitable for MLST, 21 candidate genes from 8 isolates, collected from 4 hospitals, were selected and amplified. The sequence comparisons of the isolates revealed low diversity in housekeeping genes among the *H. cinaedi* isolates. In fact, the majority of the genes tested in this preliminary experiment had high homology. Of the 21 genes investigated, 5 genes were found to have 100% homology between the 8 isolates, while only 1 polymorphism site was detected in 4 genes. For example, the allele of the *yphC* gene, which encodes the GTP-binding protein, was found to be identical in all isolates. Of the 21 genes examined from the 8 *H. cinaedi* isolates, 7 genes were found to have relatively high diversity and were selected for use in the MLST analysis (Table 1).

Characteristics of MLST genes in *H. cinaedi* isolates. Genes from all of the clinical isolates and the 6 reference strains were successfully amplified and analyzed in this study. The characteristics of the 7 loci identified as being suitable for MLST are described in Table 2. These loci have lengths ranging between 411 and 658 bp, with a total composite length of 3,806 bp. The number of variable sites present in each allele ranged from 3 (*tkt*) to 21 (*aroE*), and the allele number for each gene ranged from 3 (*cdtB*) to 6 (*aroE*).

Sequence types of *H. cinaedi*. The 50 clinical isolates and the 6 reference strains were classified into 14 STs using the MLST method described in this study. The allelic profiles of the STs are presented in Table 2. Following eBURST analysis, ST1, ST2, and ST3 were defined as CC1. Similarly, ST4, ST5, and ST6 were assigned to CC4, while ST9, ST10, and ST11 formed CC9. Accordingly, the 56 isolates and reference strains were classified into 8 CCs. The phylogenetic tree for these strains is shown in Fig. 1. The phylogeny was estimated using concatenated sequences comprising the 7 loci (23S rRNA, *ppa*, *aspA*, *aroE*, *atpA*, *tkt*, and *cdtB*) with statistical support for the nodes being assessed via the bootstrap resampling method with 1,000 resamplings.

Relationship between the sequence types of *H. cinaedi* isolates and the hospitals from which they were isolated, including clinical manifestations. *H. cinaedi* isolates were collected from 7 hospitals in Japan, and the distribution of STs in each hospital was compared (Table 3). Of the 12 isolates from hospital A, obtained over 3 months within the same ward, 11 isolates were CC9 [ST10 ($n = 3$), ST11 ($n = 8$)] and 1 isolate was CC1 (ST2). Both isolates from hospital B, isolated in the same ward over a 1-month period, were demonstrated to belong to the same ST, CC4 (ST4). Six isolates from hospital D, obtained sporadically between 2003 and 2008, revealed CC1 [ST3 ($n = 2$)], CC4 [ST5 ($n = 1$), ST6 ($n = 1$)], and CC9 [ST10 ($n = 2$)]. Clinical manifestations were available for 26 isolates and no relationships were identified between clonal complexes (STs) and patient age, diseases, and *H. cinaedi*-isolated clinical materials. The 3 isolates belonging to CC1 [ST2 ($n = 1$), ST3 ($n = 2$)] were isolated from female patients; however, CCUG18818 and CCUG18819 belonged to CC1 (ST1) and were reportedly isolated from male patients. All other isolates, belonging to CC4, CC8, and CC9, were isolated more frequently from male patients (the male/female ratios were 4/1, 5/0, and 10/3 in isolates belonging to CC4, CC8, and CC9, respectively). The 6 reference strains revealed different STs, compared to the Japanese isolates, except for CCUG43521 (from Australia), which was classified as CC4 (ST4), the same ST as the isolates from hospital B in Japan.

PFGE patterns of *H. cinaedi* and relationship with sequence types. PFGE was performed on the 18 culturable clinical isolates

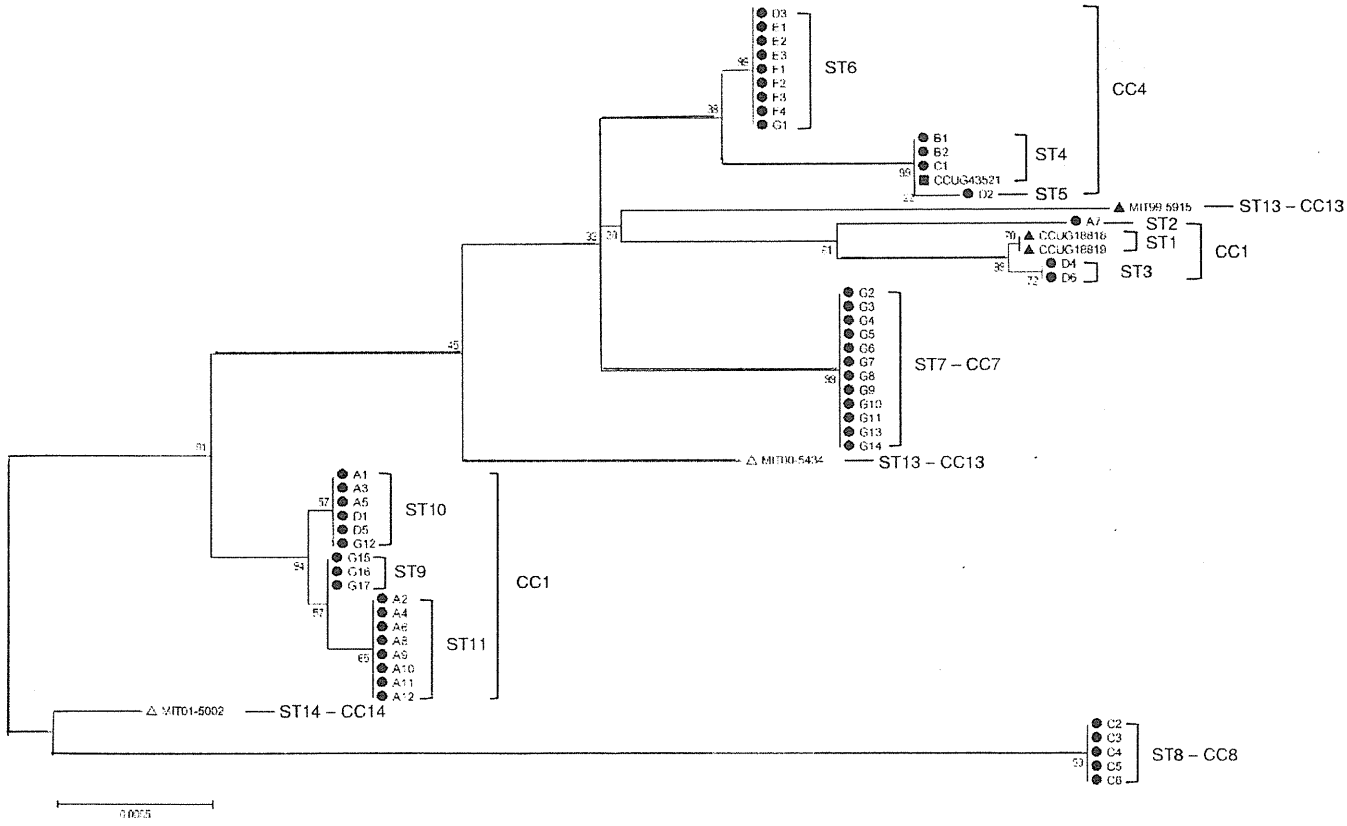

FIG 1 Genetic relationship of sequence types among 50 *H. cinaedi* isolates from 7 hospitals in Japan and 6 reference strains. The phylogenic tree was constructed using the neighbor-joining method with MEGA (version 5.05) (27) software and the maximum composite likelihood model, with statistical support for the nodes being assessed via the bootstrap resampling method with 1,000 resamplings. The letter in each isolate's identifier indicates the hospital at which the strain was isolated (e.g., A1 to A12 were isolated from hospital A). ●, human isolates from Japan; ▲, human isolates from the United States; ■, human isolates from Australia; △, rhesus monkeys isolates from the United States; ST, sequence type; CC, clonal complex.

and the 6 reference strains (Fig. 2). Based on the genomic information for CCUG18818 (available in the NCBI database), XhoI was chosen as the restriction enzyme because it cleaves chromosomal DNA less frequently. Seventeen of 18 isolates and 3 reference strains (CCUG43521, MIT 00-5434, and MIT 01-5002) were typed by XhoI digestion. Isolate A7, the CC1 [ST2] isolate obtained from hospital A, was not digested by XhoI, and similarly, CCUG18818 [CC1 (ST1)], CCUG18819 [CC1 (ST1)] and MIT 99-5915 [CC13 (ST13)] were nontypeable by XhoI digestion. SpeI digestion, which has been used for DNA digestion for PFGE analysis of *H. cinaedi* (13), was also tested, and all isolates were digested, though many small bands appeared.

TABLE 3 Prevalence of STs among *H. cinaedi* isolates from 7 hospitals in Japan

Strains	Hospital or host	City or country	No. of isolates	Clonal complex [sequence type (no. of isolates)]
Clinical isolates from Japan (n = 18)	A	Sapporo	12	CC1 [ST2 (1)], CC9 [ST10 (3), ST11 (8)]
	B	Tokyo	2	CC4 [ST4 (2)]
	C	Tokyo	6	CC4 [ST4 (1)], CC8 [ST8 (5)]
	D	Tokyo	6	CC1 [ST3 (2)], CC4 [ST5 (1), ST6 (1)], CC9 [ST10 (2)]
	E	Tokyo	3	CC4 [ST6 (3)]
	F	Tokyo	4	CC4 [ST6 (4)]
	G	Tokyo	17	CC4 [ST6 (1)], CC7 [ST7 (12)], CC9 [ST9 (3), ST10 (1)]
Reference strains				
CCUG18818	Human	USA	1	CC1 [ST1]
CCUG18819	Human	USA	1	CC1 [ST1]
CCUG43521	Human	Australia	1	CC4 [ST4]
MIT 99–5914	Human	USA	1	CC12 [ST12]
MIT 00–5433	Rhesus monkey	USA	1	CC13 [ST13]
MIT 01–5001	Rhesus monkey	USA	1	CC14 [ST14]

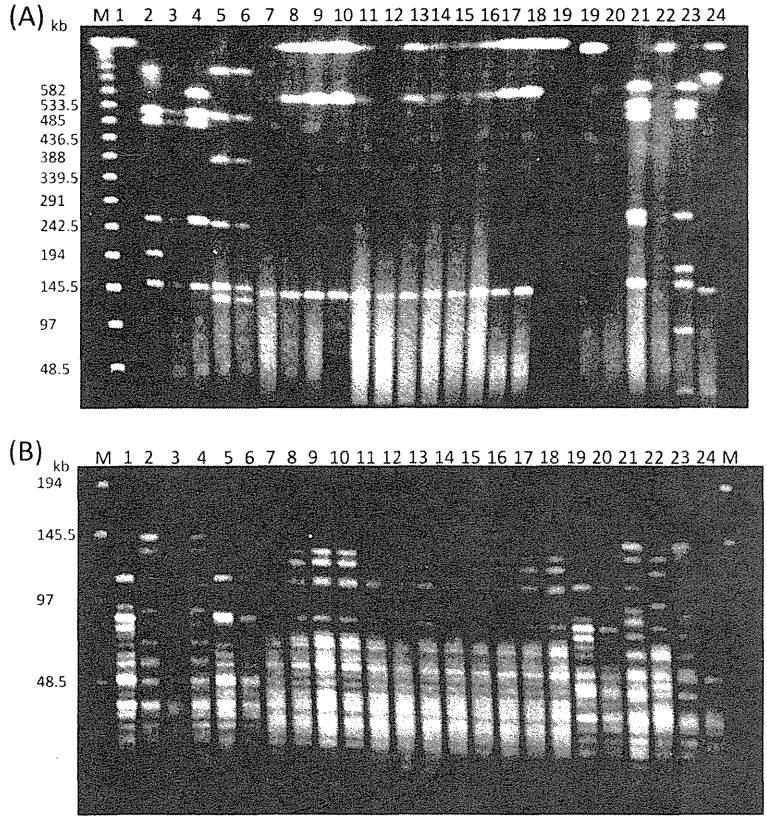

Lane	Isolate	Sequence type	Clonal Complex
1	A7	2	1
2	F1	6	4
3	F2	6	4
4	F4	6	4
5	G13	7	7
6	G14	7	7
7	G15	9	9
8	G17	10	9
9	A1	10	9
10	A3	11	9
11	A5	11	9
12	A8	11	9
13	A2	11	9
14	A4	11	9
15	A6	11	9
16	A9	11	9
17	A10	11	9
18	A11	11	9
19	CCUG18818	1	1
20	CCUG18819	1	1
21	CCUG43521	4	4
22	MIT99-5915	12	12
23	MIT00-5434	13	13
24	MIT01-5002	14	14
M	lambda marker λcl857Sam7		

FIG 2 Pulsed-field gel electrophoresis patterns of XhoI-digested (A) and SpeI-digested (B) *H. cinaedi* isolates from Japan as well as the six reference strains. The letter in each isolate's identifier indicates the hospital at which the strain was isolated (e.g., A1 to A12 were isolated from hospital A).

Of the 18 Japanese isolates (11 from hospital A, 3 from hospital F, and 4 from hospital G), 10 isolates from hospital A and 2 isolates from hospital G revealed identical PFGE patterns. These 12 isolates belonged to CC9 [ST9 (n = 2), ST10 (n = 3), ST11 (n = 7)]. Another 2 isolates from hospital G, belonging to CC7 (ST7), also revealed identical PFGE patterns. Three isolates from hospital F, belonging to CC4 (ST6), revealed similar, but not identical, patterns between isolates. Isolate A7, which belonged to CC1 (ST2), revealed a pattern similar to that of CCUG18818 and CCUG18819, which belong to CC1 (ST1). CCUG43521, which belongs to CC4 (ST4), revealed a pattern similar to that of isolates F1, F2, and F4, which belong to CC4 (ST6).

Antimicrobial susceptibilities and antimicrobial resistance genes in *H. cinaedi* isolates. The susceptibilities of 18 isolates of the *H. cinaedi* isolates from Japan as well as the 6 reference strains to the antimicrobial agents were measured. The MICs of each antimicrobial agent are shown in Table 4. Since significant differences were not observed between the MICs of amoxicillin and those of amoxicillin plus clavulanic acid, the MICs of amoxicillin are not shown in Table 4. Although the MICs of clarithromycin and ciprofloxacin were high for all isolates tested in this study (the MIC_{90}s were >128 mg/liter and 128 mg/liter for clarithromycin and ciprofloxacin, respectively), the MICs of imipenem, minocycline, and gentamicin were relatively low (the MIC_{90}s for imipenem, minocycline, and gentamicin were 0.125 mg/liter, 0.125 mg/liter, and 0.5 mg/liter, respectively). Although the breakpoints for *H. cinaedi* have yet to be determined, these isolates were obvi-

TABLE 4 Antimicrobial susceptibilities of 18 *H. cinaedi* isolates from Japan and 6 reference strains

Strain	Host, country, yr of isolation	MIC (μg/μl) of[a]: Amoxicillin + clavulanic acid	Imipenem	Clarithromycin	Ciprofloxacin	Minocycline	Gentamicin
Clinical isolates (n = 50)	Human, Japan, 2003–2008	0.5–8 (8)	0.031–0.125 (0.125)	16–>128 (>128)	16–128 (128)	0.016–0.25 (0.125)	0.125–1 (0.5)
CCUG18818	Human, USA, 1986	8	0.063	0.008	0.25	0.25	0.25
CCUG18819	Human, USA, 1986	4	0.031	4	0.125	0.125	0.5
CCUG43521	Human, Australia, 2000	4	0.031	128	0.125	0.125	0.5
MIT 99–5915	Human, USA, 1999	0.5	0.016	>128	0.063	0.031	0.125
MIT00–5434	Rhesus monkey, USA, 2000	4	0.031	0.031	16	0.063	0.5
MIT 01–5002	Rhesus monkey, USA, 2000	4	0.031	0.031	8	0.031	0.5

[a] Values for the Japanese clinical isolates are ranges (MIC_{90}s).

ously resistant to clarithromycin and ciprofloxacin (3, 17). To identify the mechanism of this resistance, the 23S rRNA and *gyrA* genes of all isolates were sequenced. The isolates from Japan revealed a mutation from adenine to guanine at position 2018 in the *H. cinaedi* 23S rRNA; the numbering is according to the DNA sequence of the 23S rRNA gene of CCUG18818 (accession no. AY596254). Three of the six reference strains, CCUG18818, MIT00-5434, and MIT01-5002, did not demonstrate a mutation at position 2018, and clarithromycin MICs ranged from 0.008 to 0.031 mg/liter. However, CCUG18819, CCUG43521, and MIT99-5915 revealed an adenine-to-guanine mutation at position 2018, and their MICs ranged from 4 to >128 mg/liter. MIT99-5915 (MIC, >128 mg/liter) revealed an additional adenine-to-cytosine mutation at position 2017. DNA sequencing of the *gyrA* genes of ciprofloxacin-resistant *H. cinaedi* isolates and the reference strains further indicated that all isolates had a threonine to isoleucine mutation at position 84 of GyrA, the numbering is according to the amino acid sequence of the CCUG18818 GyrA protein (accession no. ZP_07806036). Three isolates were also found to have an additional mutation at position 88, involving a mutation from aspartic acid to glycine, histidine, or asparagine.

DISCUSSION

This study attempted to identify the genes that may be used to classify *H. cinaedi* by MLST. However, the housekeeping genes of *H. cinaedi* were found to have low diversity. For example, although data obtained using the MLST analysis method developed in this study suggested that 8 isolates, which were used for the identification of suitable genes for MLST, should belong to different STs, the *yphC* gene, encoding GTP-binding protein, was found to be identical between the 8 isolates. This is unlike the situation with *H. pylori*, where *yphC* has been used for MLST analysis and has revealed a high degree of diversity among *H. pylori* isolates. A similar phenomenon was observed for the *mutY* and *trpC* genes, which were found to be unsuitable for *H. cinaedi* MLST, despite their use in MLST for *H. pylori*. Of the 7 genes used for MLST in *H. pylori*, only the *ppa* and *atpA* genes were suitable for use in the *H. cinaedi* analysis. These results indicate that, whereas *H. pylori* is a genetically diverse bacterial species, the housekeeping genes of *H. cinaedi* are highly conserved. Therefore, we analyzed other housekeeping genes that have been used for MLST analysis in *Campylobacter* spp. and other bacterial species. Of the 7 genes used for MLST in *C. jejuni*, *aspA* and *tkt* were suitable for *H. cinaedi* analysis.

A previous comparison of the 23S rRNA gene sequences of the isolates from hospital A indicated that there was a high possibility of nosocomial transmission of *H. cinaedi* between patients (18). Furthermore, 11/12 (91.7%) of the isolates identified in hospital A were found to belong to CC9 in this study, and the PFGE patterns of the isolates belonging to CC9 were identical. These results indicated that CC9 may have been prevalent in patients from hospital A. Furthermore, 12 of the 17 isolates from hospital G were ST7, and although only 4 of those isolates were available for PFGE, 2 of the isolates belonging to ST7 showed an identical pattern, and it was different from the patterns of 2 other isolates that belonged to ST9. Additionally, both isolates from hospital B, which were isolated from the same ward within a single month, revealed the same ST, CC4 [ST4]; these results suggested that nosocomial transmission of *H. cinaedi* is possible and that this organism may colonize individuals in the hospital environment.

H. pylori infection is believed to occur rarely in adults; instead, the infection is thought to be established during childhood, likely by oral transmission from an infected mother or contaminated water source (8). In contrast, the results of this study indicate that *H. cinaedi* infection may be transmissible between adults and that the possibility of nosocomial transmission between individuals should be considered, particularly among immunocompromised patients. Similarly, the isolates from hospital D represented three CCs: CC1, CC4, and CC9. These results are consistent with the fact that these isolates were obtained between 2003 and 2008 and that *H. cinaedi* infections had occurred sporadically throughout that period. When and how these patients became infected with *H. cinaedi* remains unknown; it is possible, as well, that *H. cinaedi* may have been present in a latent form in these patients and may have induced symptoms when the immune system was weakened.

Two isolates from rhesus monkeys and four human isolates from countries other than Japan were also analyzed, and all belonged to different STs than the isolates from Japan, except CCUG43521, which belonged to same ST (ST4) as the isolates from hospital B. A comparison of the CCs and STs with the PFGE patterns of the isolates indicated that the MLST results were consistent with the PFGE patterns. PFGE is a useful technique for typing the isolates, even though some isolates were nontypeable by XhoI. Generally, restriction enzymes that cleave chromosomal DNA less frequently should be selected for PFGE. HincII, which also cleaves chromosomal DNA less frequently, similar to XhoI, was also tried and was found to digest the DNA from a few isolates. All isolates were successfully digested by SpeI; however, SpeI cleaves chromosomal DNA more frequently than XhoI and HincII and is not the best restriction enzyme for PFGE. Given the limitations of PFGE analysis in *H. cinaedi*, further investigations are required, but the MLST method developed in this study may be useful for typing *H. cinaedi* isolates and for elucidating their route(s) of transmission.

The susceptibilities of multiple *H. cinaedi* isolates to various antimicrobial agents were also examined in this study. Susceptibilities to amoxicillin-clavulanic acid, imipenem, gentamicin, and minocycline showed no significant differences between the *H. cinaedi* isolates from Japan and the 6 reference strains. On the other hand, the MICs of clarithromycin for the human isolates from Japan were very high, compared to those for CCUG 18818 and the two *H. cinaedi* strains from rhesus monkeys. The mutation from adenine to guanine, identified at position 2018 in the *H. cinaedi* 23S rRNA sequence, corresponds to mutations at positions 2143 in *H. pylori* and 2059 in *E. coli*; these mutations have been proven to confer resistance to clarithromycin in these strains by removing the adenine required for macrolides to inhibit protein synthesis (29). Similarly, Kuijper et al. analyzed the 23S rRNA gene of erythromycin-susceptible and erythromycin-resistant *H. cinaedi* isolates and showed that erythromycin-resistant *H. cinaedi* strains possessed this mutation at position 2018, while no mutation was present in erythromycin-susceptible *H. cinaedi* (14). In the current study, the mutations at position 2018 corresponded to the clarithromycin resistance in all analyzed strains, and all isolates from Japan had this mutation. These results indicate that the isolates used in this study were all highly resistant to clarithromycin.

H. cinaedi isolates from humans, prior to 2000, revealed low MICs of ciprofloxacin, while MICs of ciprofloxacin were high not only for isolates from Japan but also for isolates from rhesus monkeys. DNA sequencing of the *gyrA* genes of ciprofloxacin-resistant

H. cinaedi isolates indicated that all of the isolates also had a mutation from threonine to isoleucine at position 84 of GyrA. This mutation, which corresponds to positions 87 in *H. pylori* and 83 in *E. coli*, has been shown to confer fluoroquinolone resistance on many bacterial species (10). Furthermore, 3 isolates had an additional mutation at position 88, corresponding to positions 91 and 87 in *H. pylori* and *E. coli*, respectively, which has also been shown to confer resistance. Double mutations have usually been found to confer high-level resistance to fluoroquinolone upon bacteria (10, 19, 28). Unfortunately, because of the inability to reculture 32 of the 50 *H. cinaedi* isolates from the stocks stored at −80°C, the susceptibilities of the isolates that possessed double mutations in GyrA were not measured; however, considering our data together with previous reports, the *H. cinaedi* isolates from Japan used in this study are resistant to fluoroquinolone, and in some cases the level of this resistance may be high. Finally, three isolates which possessed double mutations in GyrA in this study belonged to different STs (ST6, -10, and -11, respectively), suggesting that the relationship between STs and resistance may be weak. Further investigations using susceptible isolates are, therefore, needed. With regard to erythromycin and ciprofloxacin, Kiehlbauch et al. (11) have shown that *H. cinaedi* isolates from both humans and animals are susceptible to both of these antimicrobial agents, with MIC ranges for erythromycin and ciprofloxacin in animal-isolated *H. cinaedi* of <0.06 to 0.5 mg/liter and 0.12 to 1.0 mg/liter, respectively, and 0.06 to >128 mg/liter and 0.12 to 8.0 mg/liter in isolates from humans, respectively. Ciprofloxacin was also reported to successfully eradicate *H. cinaedi* infections in humans in 1991 and 2000 (15, 23). These results suggest that *H. cinaedi* was once susceptible to macrolides and fluoroquinolones, with the majority of *H. cinaedi* isolates gaining resistance in response to the increased use of these antimicrobials.

This study describes the use of molecular epidemiological analysis using MLST to genotype *H. cinaedi* isolates. We were able to classify 50 Japanese hospital isolates and 6 reference strains into 14 STs. The distribution of STs suggested the occurrence of nosocomial infection of *H. cinaedi* in hospitals, while in other cases, *H. cinaedi* infections occurred sporadically within a single hospital. Further analysis is needed to elucidate the epidemiology of *H. cinaedi*. All isolates had mutations in the 23S rRNA gene and GyrA, suggesting the seriousness of the increase in resistance of *H. cinaedi* isolates to clarithromycin and ciprofloxacin, in Japan.

ACKNOWLEDGMENTS

We thank the following individuals for providing the *H. cinaedi* isolates used in this study: Hiroyuki Nishiyama, Nihon University School of Medicine; Keizo Yamaguchi, Toho University; Michiko Yagoshi, Nihon University School of Medicine; Sayoko Kawakami, Teikyo University Hospital; Akiko Yoneyama, Toranomon Hospital; Shunji Takahashi, Sapporo City General Hospital; Masaya Mukai, Sapporo City General Hospital; Koichiro Minauchi, Sapporo City General Hospital. We also thank Kai Kumiko, Yoshie Taki, Yumiko Yoshimura, and Yumiko Hongo for their technical assistance.

This study was supported by a Grant-in-Aid for Scientific Research (C) from the Japan Society for Promotion of Science (no. 22590410), and a grant from the Ministry of Health, Labor and Welfare of Japan (H21-Shinkou-Ippan-008).

REFERENCES

1. **Burman WJ, Cohn DL, Reves RR, Wilson ML.** 1995. Multifocal cellulitis and monoarticular arthritis as manifestations of *Helicobacter cinaedi* bacteremia. Clin. Infect. Dis. **20**:564–570.
2. **Burucoa C, Lhomme V, Fauchere JL.** 1999. Performance criteria of DNA fingerprinting methods for typing of *Helicobacter pylori* isolates: experimental results and meta-analysis. J. Clin. Microbiol. **37**:4071–4080.
3. **Clinical and Laboratory Standards Institute.** 2012. Methods for dilution antimicrobial susceptibility tests for bacteria that grow aerobically. Approved standard, 9th ed. CLSI, Wayne, PA.
4. **Falush D, et al.** 2003. Traces of human migrations in *Helicobacter pylori* populations. Science **299**:1582–1585.
5. **Fox JG, et al.** 2001. Isolation of *Helicobacter cinaedi* from the colon, liver, and mesenteric lymph node of a rhesus monkey with chronic colitis and hepatitis. J. Clin. Microbiol. **39**:1580–1585.
6. **Fox JG, et al.** 2009. Chronic hepatitis, hepatic dysplasia, fibrosis, and biliary hyperplasia in hamsters naturally infected with a novel helicobacter classified in the *H. bilis* cluster. J. Clin. Microbiol. **47**:3673–3681.
7. **Gebhart CJ, Fennell CL, Murtaugh MP, Stamm WE.** 1989. *Campylobacter cinaedi* is normal intestinal flora in hamsters. J. Clin. Microbiol. **27**:1692–1694.
8. **Goh KL, Chan WK, Shiota S, Yamaoka Y.** 2011. Epidemiology of Helicobacter pylori infection and public health implications. Helicobacter **16**(Suppl. 1):1–9.
9. **Holst H, et al.** 2008. A case of Helicobacter cinaedi bacteraemia in a previously healthy person with cellulitis. Open Microbiol. J. **2**:29–31.
10. **Jacoby GA.** 2005. Mechanisms of resistance to quinolones. Clin. Infect. Dis. **41**(Suppl. 2):S120–126.
11. **Kiehlbauch JA, et al.** 1995. Genotypic and phenotypic characterization of Helicobacter cinaedi and Helicobacter fennelliae strains isolated from humans and animals. J. Clin. Microbiol. **33**:2940–2947.
12. **Kiehlbauch JA, Tauxe RV, Baker CN, Wachsmuth IK.** 1994. *Helicobacter cinaedi*-associated bacteremia and cellulitis in immunocompromised patients. Ann. Intern. Med. **121**:90–93.
13. **Kitamura T, et al.** 2007. *Helicobacter cinaedi* cellulitis and bacteremia in immunocompetent hosts after orthopedic surgery. J. Clin. Microbiol. **45**: 31–38.
14. **Kuijper EJ, Stevens S, Imamura T, De Wever B, Claas EC.** 2003. Genotypic identification of erythromycin-resistant campylobacter isolates as helicobacter species and analysis of resistance mechanism. J. Clin. Microbiol. **41**:3732–3736.
15. **Lasry S, et al.** 2000. *Helicobacter cinaedi* septic arthritis and bacteremia in an immunocompetent patient. Clin. Infect. Dis. **31**:201–202.
16. **Mammen MP, Jr, Aronson NE, Edenfield WJ, Endy TP.** 1995. Recurrent *Helicobacter cinaedi* bacteremia in a patient infected with human immunodeficiency virus: case report. Clin. Infect. Dis. **21**:1055.
17. **Megraud F, Lehours P.** 2007. Helicobacter pylori detection and antimicrobial susceptibility testing. Clin. Microbiol. Rev. **20**:280–322.
18. **Minauchi K, et al.** 2010. The nosocomial transmission of *Helicobacter cinaedi* infections in immunocompromised patients. Intern. Med. **49**: 1733–1739.
19. **Miyachi H, et al.** 2006. Primary levofloxacin resistance and *gyrA/B* mutations among *Helicobacter pylori* in Japan. Helicobacter **11**:243–249.
20. **Murakami H, et al.** 2003. Isolation of *Helicobacter cinaedi* from blood of an immunocompromised patient in Japan. J. Infect. Chemother. **9**:344–347.
21. **Orlicek SL, Welch DF, Kuhls TL.** 1993. Septicemia and meningitis caused by *Helicobacter cinaedi* in a neonate. J. Clin. Microbiol. **31**:569–571.
22. **Riley LK, Franklin CL, Hook RR, Jr, Besch-Williford C.** 1996. Identification of murine helicobacters by PCR and restriction enzyme analyses. J. Clin. Microbiol. **34**:942–946.
23. **Sacks LV, Labriola AM, Gill VJ, Gordin FM.** 1991. Use of ciprofloxacin for successful eradication of bacteremia due to Campylobacter cinaedi in a human immunodeficiency virus-infected person. Rev. Infect. Dis. **13**: 1066–1068.
24. **Saunders KE, McGovern KJ, Fox JG.** 1997. Use of pulsed-field gel electrophoresis to determine genomic diversity in strains of Helicobacter hepaticus from geographically distant locations. J. Clin. Microbiol. **35**: 2859–2863.
25. **Singh A, Goering RV, Simjee S, Foley SL, Zervos MJ.** 2006. Application of molecular techniques to the study of hospital infection. Clin. Microbiol. Rev. **19**:512–530.
26. **Stauffer GV, Plamann MD, Stauffer LT.** 1981. Construction and expression of hybrid plasmids containing the Escherichia coli glyA genes. Gene **14**:63–72.
27. **Tamura K, et al.** 2011. MEGA5: molecular evolutionary genetics analysis

using maximum likelihood, evolutionary distance, and maximum parsimony methods. Mol. Biol. Evol. 28:2731–2739.
28. **Tankovic J, Lascols C, Sculo Q, Petit JC, Soussy CJ.** 2003. Single and double mutations in *gyrA* but not in gyrB are associated with low- and high-level fluoroquinolone resistance in *Helicobacter pylori*. Antimicrob. Agents Chemother. 47:3942–3944.
29. **Taylor DE, Ge Z, Purych D, Lo T, Hiratsuka K.** 1997. Cloning and sequence analysis of two copies of a 23S rRNA gene from Helicobacter pylori and association of clarithromycin resistance with 23S rRNA mutations. Antimicrob. Agents Chemother. 41:2621–2628.
30. **Taylor NS, Ge Z, Shen Z, Dewhirst FE, Fox JG.** 2003. Cytolethal distending toxin: a potential virulence factor for Helicobacter cinaedi. J. Infect. Dis. 188:1892–1897.
31. **Tee W, Street AC, Spelman D, Munckhof W, Mijch A.** 1996. *Helicobacter cinaedi* bacteraemia: varied clinical manifestations in three homosexual males. Scand. J. Infect. Dis. 28:199–203.
32. **Totten PA, et al.** 1985. *Campylobacter cinaedi* (sp. nov.) and *Campylobacter fennelliae* (sp. nov.): two new *Campylobacter* species associated with enteric disease in homosexual men. J. Infect. Dis. 151:131–139.
33. **Vandamme P, Falsen E, Pot B, Kersters K, De Ley J.** 1990. Identification of *Campylobacter cinaedi* isolated from blood and feces of children and adult females. J. Clin. Microbiol. 28:1016–1020.

Journal of Antimicrobial Chemotherapy Advance Access published February 6, 2013

Journal of Antimicrobial Chemotherapy

J Antimicrob Chemother
doi:10.1093/jac/dkt031

Detection of Tripoli metallo-β-lactamase 2 (TMB-2), a variant of bla_{TMB-1}, in clinical isolates of *Acinetobacter* spp. in Japan

Satowa Suzuki[1]*, Mari Matsui[1], Masato Suzuki[1], Akira Sugita[2], Yoko Kosuge[2], Nobuhiro Kodama[3], Yasuko Ichise[3] and Keigo Shibayama[1]

[1]*Department of Bacteriology II, National Institute of Infectious Diseases, 4-7-1 Gakuen, Musashi-Murayama Tokyo, Japan 208-0011;* [2]*Yokohama Municipal Hospital, 56 Okazawa-cho, Hodogaya Ward, Yokohama, Japan;* [3]*Fukuoka Tokushukai Medical Center, 4-5 Sugukita, Kasuga Fukuoka, Japan*

*Corresponding author. Tel: +81-42-561-0771; Fax: +81-42-561-7173; E-mail: suzukiss@nih.go.jp

Keywords: MBLs, TMB-1, carbapenemases

Sir,

Metallo-β-lactamase is an important resistance determinant among Gram-negative bacteria, and some metallo-β-lactamase genes are encoded on mobile gene elements that can spread among various clinically important bacterial species.[1] TMB-1 (Tripoli metallo-β-lactamase 1) was first identified in 2012 in an *Achromobacter xylosoxidans* strain isolated from a hospital environment sample in Tripoli, Libya.[2] Here, we report two cases in which bla_{TMB}-positive non-*baumannii Acinetobacter* spp. were isolated from patients with no history of international travel.

The first case, a carbapenem-resistant *Acinetobacter* sp. (MRY12-142) was isolated from a urine sample in December 2011. This case had no recent history of international travel. For the second case, *Acinetobacter* sp. (MRY12-226) was isolated from necrotic tissue in July 2012. This patient also had no international travel history. These two cases were identified in two hospitals that are separated by more than 1000 km, and there was no epidemiological link between the two cases.

Acinetobacter spp. were identified by sequencing the partial *rpoB* gene and the 16S–23S rRNA gene spacer region,[3,4] which revealed *Acinetobacter pittii* in the first case and *Acinetobacter* genomospecies 14BJ in the second case. Both isolates were resistant to penicillins, cephalosporins, imipenem, meropenem and trimethoprim/sulfamethoxazole, but susceptible to fluoroquinolones, amikacin, and minocycline according to MICs determined by the VITEK2 system (bioMérieux, Lyon, France) and the recommended breakpoints of CLSI 2012.[5] Metallo-β-lactamase production was screened using a disc containing sodium mercaptoacetic acid (SMA) (Eiken, Tokyo, Japan).[6] For both isolates, the growth inhibitory zone around the imipenem and ceftazidime discs expanded upon the addition of the SMA disc, which is strongly indicative of metallo-β-lactamase production.

Based on PCR analyses, both isolates were negative for bla_{NDM-1}, bla_{KPC}, bla_{IMP} bla_{VIM-1}, bla_{VIM-2}, $bla_{OXA-23-like}$, $bla_{OXA-24-like}$, $bla_{OXA-51-like}$ and $bla_{OXA-58-like}$. However, PCR analyses for class 1 integron gene cassettes, in which primers targeted the 5′-conserved region (CS) and 3′-CS, revealed two bands of ~1.2 kbp and 1.8 kbp in both isolates. Sequence analysis of the 1.2 kbp PCR products of both isolates showed that the class 1 integron gene cassette contained only one gene that had 99% amino acid identity with TMB-1, and was thus designated TMB-2. The 738 bp sequence of bla_{TMB-2} was identical to that of bla_{TMB-1}, except for one substitution at nucleotide position 544, which caused an amino acid change from serine to proline at position 228 according to the class B standard numbering[7] (GenBank accession numbers AB758277 and AB758278). Sequence analysis for the 1.8 kbp PCR product of MRY12-142 was conducted and showed that the class 1 integron gene cassette contained *aac(6′)-Ib* and a hypothetical open reading frame.

The PCR product of the class 1 integron gene cassette containing bla_{TMB-2} was ligated into pGEM-T (Promega, WI, USA) and transformed into *Escherichia coli* strain DH5α. In addition, pGEM-T harbouring bla_{TMB-1} was obtained by site-directed mutagenesis and transformed into *E. coli* DH5α to evaluate the role of this single amino acid substitution on antimicrobial susceptibility, the MICs being determined by Etest (bioMérieux). As shown in Table 1, the TMB-2-producing transformant was resistant to ceftazidime and susceptible to aztreonam, similar to the TMB-1-producing transformant. However, the TMB-2-producing transformant showed >256-fold and 16-fold lower MICs for doripenem and meropenem, respectively, compared with the TMB-1-producing transformant. The MICs of imipenem were not different for the two strains. Both transformants also showed an apparent expansion of the growth inhibitory zone around the ceftazidime disc upon addition of the SMA disc.

It has been reported that carbapenem resistance among non-*baumannii Acinetobacter* spp. is usually due to the production of metallo-β-lactamase.[8–10] To our knowledge, this study is the first to report an *Acinetobacter* spp. positive for bla_{TMB} and to identify a new variant, bla_{TMB-2}. It is also the first report to identify bla_{TMB} in clinical isolates. The low MICs of carbapenems for transformant cells suggests that additional resistance mechanisms, such as the production of other classes of β-lactamase, a reduction in outer membrane protein expressions and an acceleration of efflux pump activities, may be involved in the carbapenem resistance of parental clinical isolates of *Acinetobacter* spp. Although the same phenomenon was reported in the IMP-type,[11] it is notable that one amino acid substitution from serine to proline in TMB-2 has drastically decreased the MICs of meropenem and doripenem. As neither patient had a history of international travel nor any epidemiological link, it is possible that bla_{TMB-2} had been endemic in Japan but unrecognized because of its reduced ability to hydrolyse carbapenems. The unrecognized spread of bla_{TMB-2} could be a concern as it can turn to bla_{TMB-1} by only one nucleotide substitution. Although

Table 1. Antimicrobial susceptibility of isolates and strains determined by Etest

Antimicrobial agents	MICs (mg/L) for isolates and strains						
	A. pittii MRY12-142	*A.* genomospecies 14BJ MRY12-226	*E. coli* DH5α (pGEM-T-TMB-2)	*E. coli* DH5α (pGEM-T-TMB-1)	*E. coli* DH5α (pGEM-T)	*E. coli* DH5α	*A. pittii* ATCC 19004
Aztreonam	32	32	0.064	0.094	0.047	0.047	16
Ceftazidime	>256	>256	>256	>256	0.25	0.38	6
Imipenem	16	>32	2	1	0.38	0.38	0.25
Meropenem	>32	>32	2	32	0.064	0.064	0.75
Doripenem	>32	>32	0.064	32	0.032	0.032	0.19

this report discusses only two cases, it may be important to evaluate the spread of this emerging metallo-β-lactamase gene among non-*baumannii Acinetobacter* spp.

Acknowledgements

We thank Kumiko Kai, Yumiko Yoshimura and Yoshie Taki for technical assistance and we thank Sunao Matsubayashi and Yuki Koura for providing clinical isolates and information.

Funding

This work was supported by a grant from the Ministry of Health, Labour and Welfare of Japan (H24-Shinkou-Ippan 010).

Transparency declarations

None to declare.

References

1 Cornaglia G, Giamarellou H, Rossolini GM. Metallo-β-lactamases: a last frontier for β-lactams? *Lancet Infect Dis* 2011; **11**: 381–93.

2 El Salabi A, Borra PS, Toleman MA *et al.* Genetic and biochemical characterization of a novel metallo-β-lactamase, TMB-1, from an *Achromobacter xylosoxidans* strain isolated in Tripoli, Libya. *Antimicrob Agents Chemother* 2012; **56**: 2241–5.

3 La Scola B, Gundi VA, Khamis A *et al.* Sequencing of the *rpoB* gene and flanking spacers for molecular identification of *Acinetobacter* species. *J Clin Microbiol* 2006; **44**: 827–32.

4 Chang HC, Wei YF, Dijkshoorn L *et al.* Species-level identification of isolates of the *Acinetobacter calcoaceticus-Acinetobacter baumannii* complex by sequence analysis of the 16S-23S rRNA gene spacer region. *J Clin Microbiol* 2005; **43**: 1632–9.

5 Clinical and Laboratory Standards Institute. *Performance Standards for Antimicrobial Susceptibility Testing: Twenty-second Informational Supplement M100-S22*. CLSI, Wayne, PA, USA, 2012.

6 Shibata N, Doi Y, Yamane K *et al.* PCR typing of genetic determinants for metallo-β-lactamases and integrases carried by Gram-negative bacteria isolated in Japan, with focus on the class 3 integron. *J Clin Microbiol* 2003; **41**: 5407–13.

7 Galleni M, Lamotte-Brasseur J, Rossolini GM *et al.* Standard numbering scheme for class B β-lactamases. *Antimicrob Agents Chemother* 2001; **45**: 660–3.

8 Yamamoto M, Nagao M, Matsumura Y *et al.* Regional dissemination of *Acinetobacter* species harbouring metallo-β-lactamase genes in Japan. *Clin Microbiol Infect* 2012; doi:10.1111/1469-0691.12013.

9 Park YK, Jung SI, Park KH *et al.* Characteristics of carbapenem-resistant *Acinetobacter* spp. other than *Acinetobacter baumannii* in South Korea. *Int J Antimicrob Agents* 2012; **39**: 81–5.

10 Lin YC, Sheng WH, Chen YC *et al.* Differences in carbapenem resistance genes among *Acinetobacter baumannii*, *Acinetobacter* genospecies 3 and *Acinetobacter* genospecies 13TU in Taiwan. *Int J Antimicrob Agents* 2010; **35**; 439–43.

11 Iyobe S, Kusadokoro H, Ozaki J *et al.* Amino acid substitutions in a variant of IMP-1 metallo-β-lactamase. *Antimicrob Agents Chemother* 2000; **44**: 2023–7.

AAC
Journals.ASM.org

Structural Insights into the Subclass B3 Metallo-β-Lactamase SMB-1 and the Mode of Inhibition by the Common Metallo-β-Lactamase Inhibitor Mercaptoacetate

Jun-ichi Wachino,[a,b] Yoshihiro Yamaguchi,[c] Shigetarou Mori,[a] Hiromasa Kurosaki,[d] Yoshichika Arakawa,[a,b] Keigo Shibayama[a]

Department of Bacteriology II, National Institute of Infectious Diseases, Musashi-Murayama, Tokyo, Japan[a]; Department of Bacteriology, Nagoya University Graduate School of Medicine, Showa-ku, Nagoya, Aichi, Japan[b]; Environmental Safety Center, Kumamoto University, Chuo-ku, Kumamoto, Japan[c]; Department of Structure-Function Physical Chemistry, Graduate School of Pharmaceutical Sciences, Kumamoto University, Chuo-ku, Kumamoto, Japan[d]

A novel subclass B3 metallo-β-lactamase (MBL), SMB-1, recently identified from a *Serratia marcescens* clinical isolate, showed a higher hydrolytic activity against a wide range of β-lactams than did the other subclass B3 MBLs, i.e., BJP-1 and FEZ-1, from environmental bacteria. To identify the mechanism underlying the differences in substrate specificity among the subclass B3 MBLs, we determined the structure of SMB-1, using 1.6-Å diffraction data. Consequently, we found that SMB-1 reserves a space in the active site to accommodate β-lactam, even with a bulky R1 side chain, due to a loss of amino acid residues corresponding to F31 and L226 of BJP-1, which protrude into the active site to prevent β-lactam from binding. The protein also possesses a unique amino acid residue, Q157, which probably plays a role in recognition of β-lactams via the hydrogen bond interaction, which is missing in BJP-1 and FEZ-1, whose K_m values for β-lactams are particularly high. In addition, we determined the mercaptoacetate (MCR)-complexed SMB-1 structure and revealed the mode of its inhibition by MCR: the thiolate group bridges to two zinc ions (Zn1 and Zn2). One of the carboxylate oxygen atoms of MCR makes contact with Zn2 and Ser221, and the other makes contact with T223 and a water molecule. Our results demonstrate the possibility that MCR could be a potent inhibitor for subclass B3 MBLs and that the screening technique using MCR as an inhibitor would be effective for detecting subclass B3 MBL producers.

The emergence of β-lactamases capable of hydrolyzing carbapenem antibiotics, i.e., carbapenemases, is of substantial concern in clinical settings since carbapenem is an important tool for the treatment of infectious diseases caused by pathogenic Gram-negative bacteria (GNB) (1). Metallo-β-lactamase (MBL; class B β-lactamase) is one of the prevalent carbapenemases among the pathogenic GNB. MBLs commonly contain one or two zinc ions in the active site and are further subdivided into three subclasses—B1, B2, and B3—based on their primary zinc binding motifs (2).

To date, a variety of MBL genes have been discovered on the chromosomes of human opportunistic and environmental bacteria, for example, L1 from *Stenotrophomonas maltophilia* (3), IND from *Chryseobacterium indologenes* (4), Sfh-1 from *Serratia fonticola* (5), CcrA from *Bacteroides fragilis* (6), CAU-1 from *Caulobacter crescentus* (7), and BJP-1 from *Bradyrhizobium japonicum* (8). On the other hand, horizontally acquired MBL genes, such as bla_{IMP} (9), bla_{VIM} (10), bla_{NDM} (11), bla_{SPM} (12), bla_{GIM} (13), and bla_{SIM} (14), have mainly been found on the plasmids of members of the family *Enterobacteriaceae*, *Pseudomonas* spp., and *Acinetobacter* spp.

We recently identified a novel subclass B3 MBL, named SMB-1, from a human opportunistic bacterium, *Serratia marcescens*, which was isolated from the urine of an inpatient in a Japanese hospital (15). SMB-1 can hydrolyze a variety of β-lactam antibiotics, including penicillins, cephalosporins, and carbapenems, as efficiently as the other subclass B3 MBLs, L1, and GOB-1 of *Elizabethkingia meningoseptica* (16, 17). On the other hand, despite belonging to the same subclass B3 MBL group, the enzymes BJP-1, CAU-1, THIN-B (of *Janthinobacterium lividum*), and FEZ-1 (of *Fluoribacter gormanii*) from environmental bacteria, have high K_m values for various β-lactams, resulting in very low affinities for the substrates and thus low catalytic efficiency (k_{cat}/K_m) (7, 8, 18, 19). There is a significant difference in hydrolytic activity against β-lactams between subclass B3 MBLs from human opportunistic bacteria and those from environmental bacteria.

Most of the subclass B3 MBL genes identified thus far were intrinsically located on the chromosomes of human opportunistic and environmental bacteria (3, 7, 8), whereas two subclass B3 MBLs, SMB-1 and AIM-1, which are predicted to be incorporated into pathogenic bacteria via mobile genetic element, were reported quite recently (15, 20). The SMB-1 gene was hypothesized to have been incorporated into the chromosome of the *S. marcescens* strain from an unknown bacterial species, via an ISCR1 element, which was previously identified to be involved in the dissemination of a variety of antibiotic resistance genes (15, 21). These indicate the possibility that not only subclass B1 MBLs, such as IMP-type, VIM-type, and NDM-type MBLs, but also subclass B3 MBLs, such as SMB-1 and AIM-1, could become widely distributed among pathogenic bacteria, resulting in a serious clinical threat.

Many techniques of screening for MBL producers are available in routine clinical microbiology settings; however, the application

Received 18 June 2012 Returned for modification 11 August 2012
Accepted 7 October 2012
Published ahead of print 15 October 2012
Address correspondence to Jun-ichi Wachino, wachino@nih.go.jp.

doi:10.1128/AAC.01264-12

of these techniques has been evaluated mainly for subclass B1 MBL producers and has not been fully evaluated for subclass B3 MBL producers. In Japan, a phenotypic method, based on a β-lactam–sodium mercaptoacetate (MCR) synergy test, is frequently used for detecting MBL producers (22, 23). We previously reported that this synergy test showed a positive result for the SMB-1-producing strain (15), but its mode of inhibition remained unknown.

In order to understand the mechanism underlying substrate preferences observed among the subclass B3 MBLs, we determined the crystal structure of SMB-1, which has a broad-spectrum substrate specificity. We also obtained the SMB-1 structure complexed with MCR and demonstrated its mode of inhibition.

MATERIALS AND METHODS

Protein expression and purification. The expression of SMB-1 (GenBank accession no. AB636283) and its purification were performed according to previously described methods (15).

Crystallization. Crystallization of SMB-1 was performed as previously described (24). In brief, 3 μl of purified protein (15 mg/ml) and 3 μl of reservoir solution were mixed and equilibrated against 500 μl of reservoir solution at 293 K, using the hanging-drop vapor-diffusion method. Two types of crystals were prepared in the present study. One (native-1a) was obtained with the reservoir solution consisting of 0.2 M ammonium sulfate, 0.1 M sodium acetate trihydrate (pH 5.3), and 28% (wt/vol) PEG monomethyl ether (MME) 2000 (reservoir A). A second type of crystal (native-1b) was obtained using a reservoir solution consisting of 1 M lithium chloride, 0.1 M MES (morpholineethanesulfonic acid; pH 6.0), and 26% (wt/vol) PEG 6000 (reservoir B). Both crystals were grown within 1 week to a size suitable for collecting diffraction data. Crystals in a complex with MCR were obtained by soaking native-1b crystals in reservoir solutions containing 10 mM sodium MCR for 1 h.

Data collection and refinement. All diffraction data were collected at 100 K on a Beamline BL-5A at the Photon Factory (PF) and NW12A at the Photon Factory Advanced Ring (PF-AR) (High Energy Accelerator Research Organization, Tsukuba, Japan). The collected diffraction data were processed and scaled using the HKL-2000 program package (25).

The structure of native SMB-1 was initially solved using the data for the native-1a crystal by molecular replacement using the MOLREP program (26) in the CCP4 suite (27). The structure of L1 MBL that had been solved using 1.7-Å resolution diffraction data (PDB code 1SML) was modified by the deletion of water molecules, zinc ions, and several loop structures; mismatched amino acids were replaced with alanine. Molecular replacement was performed by using the modified L1 structure as the search model. The Coot program was used for model building (28), and the refinement was carried out using the REFMAC5 program (29), a component of the CCP4 suite (27).

The structures of native-1b and the SMB-1–MCR complex were solved by molecular replacement using the native structures determined from the crystal native-1a, and refined by the procedures described above. The quality of each finally refined model was assessed using the program PROCHECK (30) in the CCP4 suite (27). The data collection and refinement statistics are shown in Table 1.

Site-directed mutagenesis of bla_{SMB-1} and purification of mutant proteins. Site-directed mutagenesis was performed on the pCL-SMB plasmid (15), carrying the bla_{SMB-1} gene, with the Prime STAR mutagenesis basal kit (TaKaRa, Japan). Thereafter, the mutated gene was amplified by PCR, and the fragment was ligated into a pET30a vector (Novagen, Germany). Overexpression and purification of the mutant protein was performed according to a previously described method (15).

Kinetic parameters. The steady-state constants K_m and k_{cat} were determined according to a method described previously (15). The K_i value was determined using 100 μM nitrocefin as the reporter substrate.

TABLE 1 Data collection and refinement statistics[c]

Parameter	Native	Mercaptoacetate complex
Data collection		
Beam line	BL-5A (PF)	NW12A (PF-AR)
Wavelength (Å)	1.00	1.00
Resolution range (Å)	50.0–1.60 (1.63–1.60)	50.0–2.20 (2.24–2.20)
Space group	$P3_1$	$P3_1$
Cell dimensions (Å)		
a	67.83	67.03
b	67.83	67.03
c	48.67	46.79
No. of unique reflections	32,909 (1,654)	11,951 (621)
Redundancy	11.2	11.3
Completeness (%)	99.4 (100.0)	100.0 (100.0)
R_{merge}[a] (%)	5.1 (21.6)	9.7 (29.0)
Mean I/σ (I)	73.4 (17.3)	48.2 (15.6)
V_M[b] (Å^3 Da^{-1})	2.33	2.19
Solvent content (%)	47.3	43.8
Refinement		
Resolution (Å)	27.8–1.60 (1.64–1.60)	58.1–2.20 (2.26–2.20)
No. of reflections used	31,222 (2,313)	11,367 (873)
$R_{working}$ (%)	16.5 (21.0)	16.7 (16.4)
R_{free} (%)	20.0 (27.1)	22.4 (29.4)
No. of atoms		
Protein	1921	1907
Ligand/ion	53	9
Water	277	146
B-factors (Å^2)		
Protein	19.3	27.8
Ligand/ion	35.5	25.6
Water	31.3	29.6
RMSD		
Bond length (Å)	0.011	0.008
Bond angle (°)	1.43	1.18

[a] $R_{merge} = \sum_{hkl}\sum_{n}|I_i(hkl) - \langle I(hkl)\rangle|/\sum_{hkl}\sum_{n} I_i(hkl)$, where $I_i(hkl)$ is the observed intensity for reflection for *hkl*, and $\langle I(hkl)\rangle$ is the average intensity calculated for reflection *hkl* from replicate data.

[b] V_M, Matthews coefficient.

[c] Values in parentheses are for the highest-resolution shell.

Susceptibility testing. Susceptibility testing was performed according to Clinical and Laboratory Standards Institute (CLSI) guidelines (31).

Protein data bank accession numbers. The atomic coordinates and structural factors of native SMB-1 and the SMB-1-MCR complex have been deposited in the Protein Data Bank under accession numbers 3VPE and 3VQZ, respectively.

BBL and amino acid sequence numbers. The amino acid residues of SMB-1 were assigned with BBL and amino acid sequence numbers by putting the latter number in square brackets, e.g., "R37[3]," while those of MBLs other than SMB-1 were assigned with the BBL number only (32).

RESULTS AND DISCUSSION

Overall structure of SMB-1 and its complex with MCR. The MBL SMB-1 was crystallized using two different reservoir solutions (reservoirs A and B in Materials and Methods). Both crystals (native-1a and native-1b) diffracted to 1.6 Å and belonged to the trigonal space group $P3_1$, with one molecule per asymmetric unit. Both of the finally refined structures commonly contained the residues from R37[3] to K309[261] out of the matured SMB-1 (the 262 amino acids from Q35[1] to R310[262]) and two zinc ions with a full occupancy in the active site (Fig. 1). The superpo-

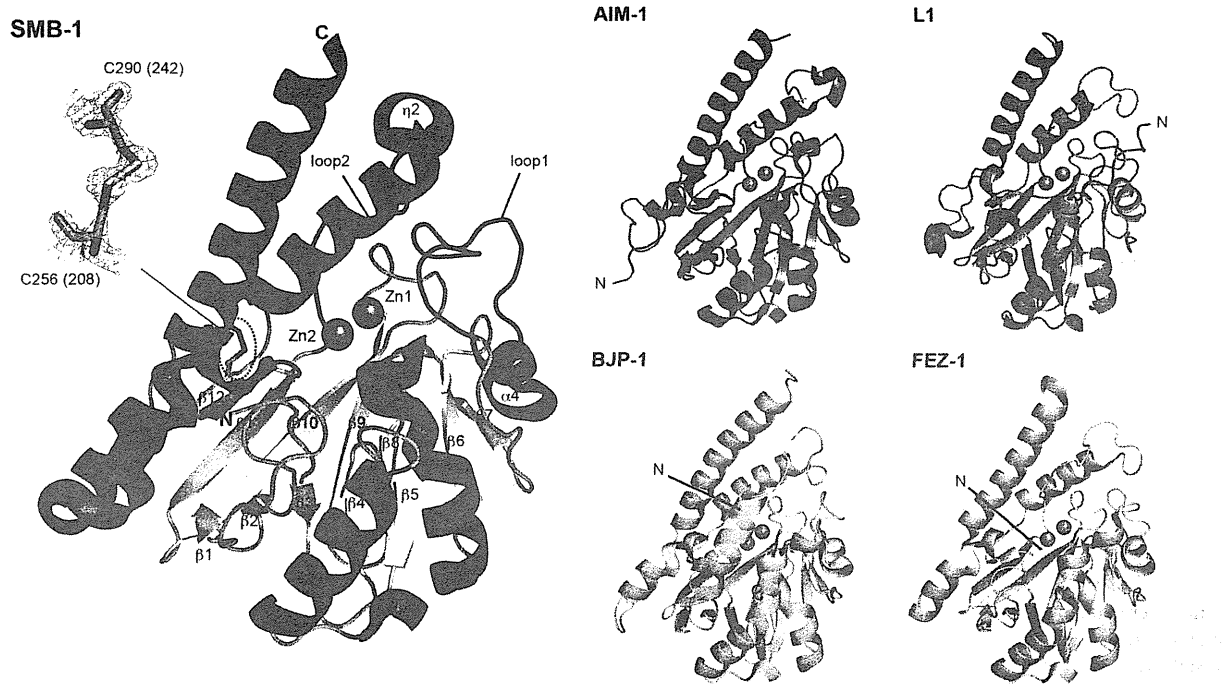

FIG 1 Schematic representation of the overall structure of SMB-1 and those of the other subclass B3 MBLs, AIM-1 (PDB code 4AWY, slate-blue), L1 (PDB code 1SML, orange), BJP-1 (PDB code 3LVZ, cyan), and FEZ-1 (PDB code 1K07, light pink). In the structure of SMB-1, the α-helices are shown in red, the β-strands are shown in yellow, and the loop region is shown in green. The two loops (loop1 and loop2) covering the active site are shown in blue. The two zinc ions are shown as gray spheres. The disulfide bond is circled with dashed lines and enlarged at the side. The figures were drawn with PyMOL.

sition of C^{α} atoms from the two native structures gave the root mean square deviation (RMSD) of 0.2 Å, indicating that the three-dimensional structures of two molecules are almost identical, with no substantial conformational differences. Unless otherwise noted, all subsequent descriptions referring to the native SMB-1 structure originate from the structure determined using the native-1a crystal data, because this yielded superior $R_{working}$ and R_{free} values of 0.17 and 0.20, respectively. A Ramachandran plot revealed that most of the residues (98.1%) are positioned in the favored region, and 1.9% residues are in the allowed region.

Next, we attempted to make SMB-1–MCR complex crystals by soaking the native crystals in reservoir solution containing sodium MCR. Diffraction data suitable for structural analysis were obtained only when soaking native-1b crystals, not native-1a crystals, despite repeated attempts. Similar to the native structure, SMB-1–MCR complex crystals belonged to the trigonal space group $P3_1$, with one molecule per asymmetric unit, and contained residues R37[3] to K309[261] and two zinc ions, as did the native structure, but with the exception of S160[116] and L161[117] (Fig. 2), which were disordered in the electron density map and were missing from the final model. The RMSD value between C^{α} atoms from the native SMB-1 and SMB-1–MCR complex was 0.3 Å, although the structure of the SMB-1–MCR complex was finally refined to 2.2 Å, which is lower than that of the native structure. The details of the data collection, crystallographic statistics of the structure determination, and refinements are shown in Table 1.

The overall structure of native SMB-1 is shown in Fig. 1. The SMB-1 structure contains 7 α-helices and 12 β-strands which form an αβ/βα sandwich structure, a common feature observed in β-lactam-hydrolyzing MBLs (33). The active site of SMB-1 was located at the bottom of a shallow cleft formed by the facing β-sheets; one sheet (N-terminal) consists of seven antiparallel strands (β1-β7), while the other (C-terminal) is composed of five antiparallel strands (β8-β12). The basis of the active site of SMB-1 was typically coordinated by two zinc ions (Zn1 and Zn2). Two loops connecting helix α4 and strand β7 (loop1), and strand β11 and helix α5 (loop2), which are typical features of subclass B3 MBLs, cover the center active-site cavity. A disulfide bridge is formed by residues C256[208] and C290[242] (Fig. 1), and the interaction pulled the last long helix α7 to the core domain of the protein. This disulfide bridge has also been observed in the other subclass B3 MBLs, AIM-1, L1, and FEZ-1, but not in BJP-1 (20, 34–36).

Coordination mode of active site. The active site in SMB-1 has two zinc ions (Zn1 and Zn2) separated by 3.5 Å (Fig. 3A). The zinc coordination mode of SMB-1 was similar to that of BJP-1 (34), whose structure was determined from high-resolution diffraction data (1.4 Å). Zn1 was coordinated to three histidine residues (H116[72], H118[74], and H196[150]) and the bridging hydroxide oxygen atom (Wat1) in a distorted tetrahedral geometry. Wat1 is assumed to contribute as the attacking nucleophile on the carbonyl carbon of the β-lactam ring. The bridging hydroxide anion is slightly asymmetrical with Zn-O distances being 2.0 and 2.1 Å for Zn1 and Zn2, respectively. The Zn1-Zn2 distance (3.5 Å) and the Zn1-OH^- (Wat1)-Zn2 angle (117°) are close to the corresponding distance (3.5 Å for subunit A and 3.4 Å for subunit B) and angle (119° for subunit A and 121° for subunit B) in BJP-1 (34). The Zn1-His distances are in the range of 2.0 to 2.1 Å (Table 2). The ranges of the His-Zn1-His and His-Zn1-O angles are 99° to 101° and 113° to 123°, respectively, and there is a significant distortion from the tetrahedral angle of 109.5°. This distortion may result from zinc ion d^{10} configuration due to the lack of ligand field stabilization.

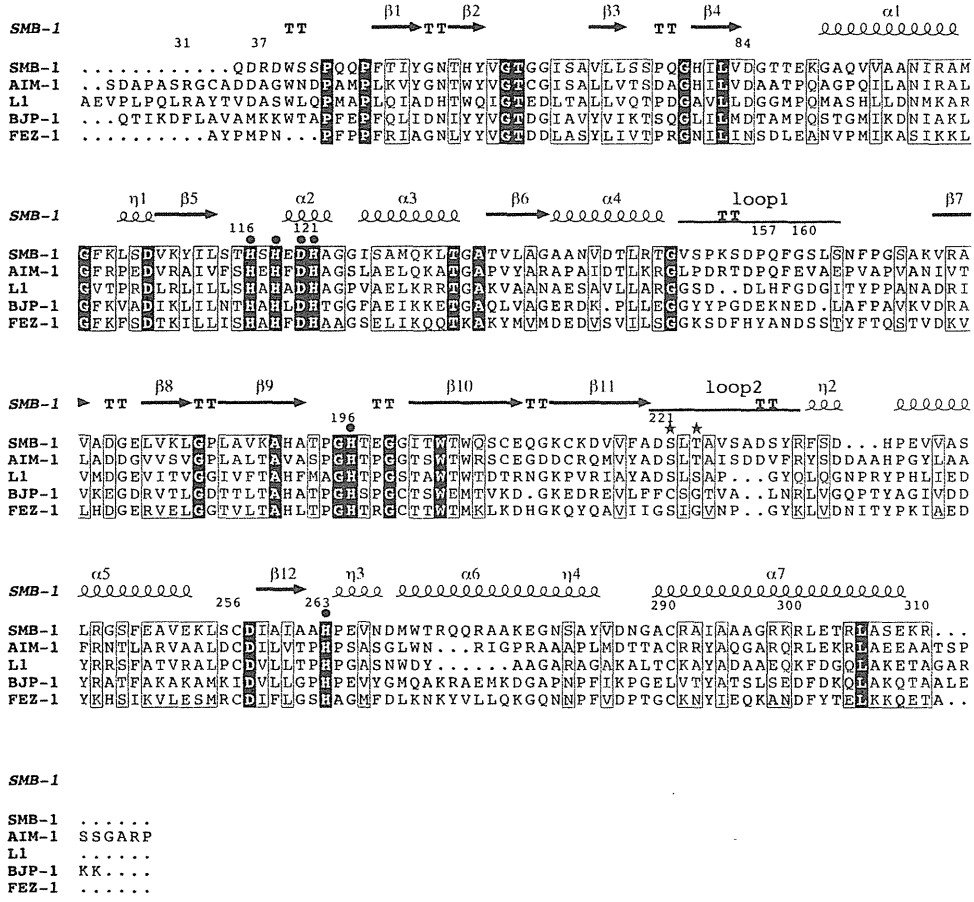

FIG 2 Amino acid alignment of the subclass B3 MBLs, SMB-1, AIM-1, L1, BJP-1, and FEZ-1 protein sequences. The strictly conserved amino acid residues are boxed in red. Physicochemically similar amino acids are shown in red. Closed circles indicate the amino acids involved in binding zinc ions. Stars indicate the residues binding to MCR. The secondary structure elements of SMB-1 are shown above the alignments. The figure was prepared using CLUSTAL W and ESPript.

In the Zn2 site, the geometry around Zn2 can be regarded as a distorted square pyramid with H263[215], D120[76], the bridging hydroxide oxygen atom (Wat1), and Wat2 on the equatorial base and H121[77] at the apex (Fig. 3A). The value of the stereochemical τ parameter (37), which could discriminate between a square pyramid ($\tau = 0$) and trigonal bipyramid ($\tau = 1$), is 0.37 {$\tau = [\beta\text{-}\alpha]/60$, where $\alpha = 144°$ for O (Wat1)-Zn2-H263[215] NE2 and $\beta = 166°$ for O (Wat2)-Zn2-D120[76] OD2}. The Zn2-ligand distances are in the range of 2.1 to 2.2 Å, in which Wat2 is tightly bound to Zn2 (2.2 Å), compared to the corresponding distance (2.5 Å) in BJP-1 (34). It must be pointed out that one of the carboxylate oxygen atoms of D120[76] is also involved in hydrogen bonding to the bridging hydroxide oxygen atom (Wat1), suggesting that D120[76] may be particularly important not only in orientating an OH^- acting as a nucleophile to the carbonyl carbon on the β-lactam ring but also in positioning the Zn2 and H263[215], as seen also in the subclass B1 and B3 MBLs (38–40). These results suggested that SMB-1 has the ability to keep the coordination geometry closer to the transition state through distortion of the regular geometry.

Structural comparison with other subclass B3 MBLs. The structure of SMB-1 and those of other subclass B3 MBLs, *viz.*, AIM-1 (PDB code 4AWY), BJP-1 (PDB code 3LVZ), L1 (PDB code 1SML), and FEZ-1 (PDB code 1K07), which have 44, 28, 32, and 29% amino acid identities to SMB-1, respectively, were compared (Fig. 2). These five proteins shared very close protein folds, as reflected by RMSD values of 1.4 to 1.9 Å (Fig. 1). On the other hand, some remarkable structural differences were observed. The secondary structures of the N termini of SMB-1, AIM-1, and L1 consist of random coil, whereas BJP-1 has an α-helix in its N-terminus region (Fig. 1). The N-terminus region of SMB-1 was much shorter than those of the other subclass B3 MBLs, although the N-terminal regions aligned well from residue W39[5] in SMB-1, AIM-1, L1, and BJP-1. Site-directed mutagenesis approaches have previously revealed that the W39 residue could influence the recognition of β-lactams in subclass B3 MBLs (41). We propose that the difference in the structure of the N termini produces differences in the hydrolytic activity of subclass B3 MBLs, such that SMB-1, AIM-1, and L1 from human opportunistic pathogens have a higher catalytic efficiency (k_{cat}/K_m) against β-lactams, whereas FEZ-1 and BJP-1, derived from environmental bacteria, have relatively lower k_{cat}/K_m values (8, 15, 16, 18, 20).

Docquier et al. have shown that the low affinities exhibited by BJP-1 for various β-lactams could be attributed to the presence of amino acid residues, like F31, in the N-terminal helix, which results in a narrower space in the active site for the binding of the β-lactams, by occupying a space in which the R1 side chain of β-lactam is assumed to be primarily positioned (Fig. 1 and 4) (34).

On the other hand, the innate N-terminus region of SMB-1 is much shorter than that of BJP-1; this would make it possible to

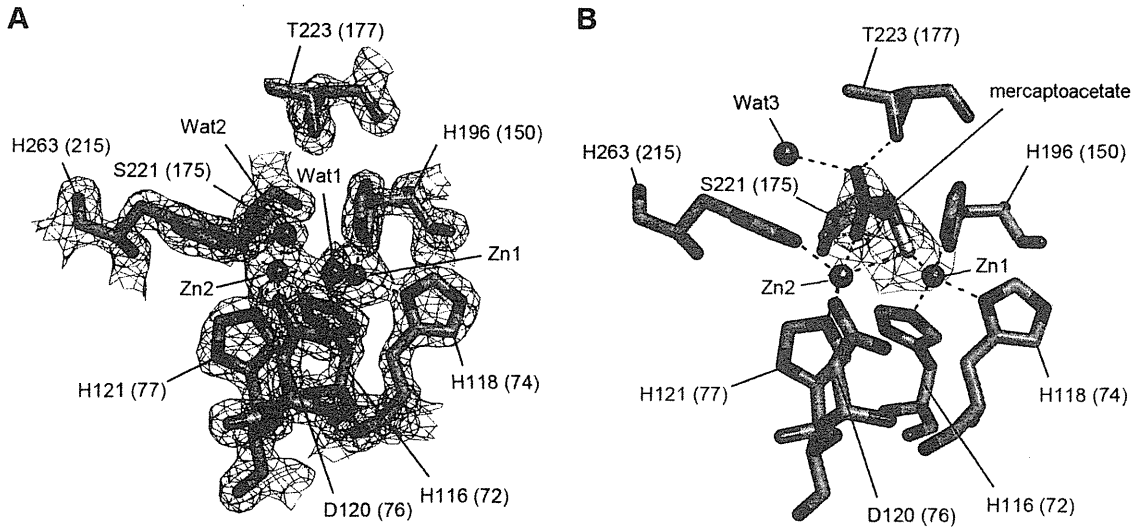

FIG 3 (A) Representation of the active site of native SMB-1. The zinc ions and water molecules are shown as gray and red spheres, respectively. The residues involved in the binding of the zinc ions are shown as green (carbon), blue (nitrogen), and red (oxygen) sticks. The electron density map (gray mesh) is shown countered at the 1.0σ level in the $2|Fo| - |Fc|$ map. The coordinate bonds around the zinc ions are shown as magenta dotted lines. The hydrogen bonds are shown as black dotted lines. (B) Representation of the active site of SMB-1 in complex with MCR. The MCR molecule is shown with magenta (carbon), yellow (sulfur), and red (oxygen) sticks. The zinc ions, zinc-binding residues, and the electron density map are shown with the color code used in panel A. The coordinate bonds around the zinc ions and the hydrogen bonds are shown as magenta and black dotted lines, respectively. The figures were drawn with PyMOL.

reserve a space for accommodating a wide range of β-lactams, even those with a bulky R1 side chain (Fig. 4). The broader substrate specificity observed in SMB-1 may thus partially depend on the space created by the loss of a long N-terminus structure that includes the residues interfering with substrate binding. AIM-1 and L1 have a long N-terminus structure similar to that of BJP-1, but their conformations and orientations largely differ from that of BJP-1 (Fig. 1). Both the N terminus of AIM-1 and that of L1 extend outward from the active site, avoiding narrowing of the space for substrate binding, and resulting in the creation of a space for accommodating β-lactams.

Structural comparison between subclass B3 MBLs, with a focus on the loop regions around the active site. The two loop regions (loop1 and loop2) were commonly considered to cover the active-site cavity in the subclass B3 MBLs (Fig. 5A). The two loops of SMB-1 adopt a very similar conformation to those of AIM-1, although loop2 in AIM-1 was partially disordered, but the conformation differed markedly compared to that of the other subclass B3 MBLs: L1, BJP-1, and FEZ-1. Loop1 (hairpin loop) and loop2 of SMB-1 and AIM-1 were spatially closer together than those of any other subclass B3 MBLs (Fig. 5A).

TABLE 2 Zinc(II)-ligand distances

Zn atom	Atom or molecule	Distance (Å)	
		Native	MCR complex
Zn1	H116[72] NE2	2.1	2.1
	H118[74] ND1	2.1	2.0
	H196[150] NE2	2.0	2.1
	O (Wat1)	2.0	
	O (Wat2)	3.1	
	O2 (MCR)		3.1
	S (MCR)		2.2
Zn2	D120[76] OD2	2.1	2.1
	H121[77] NE2	2.1	2.0
	H263[215] NE2	2.1	2.0
	O (Wat1)	2.1	
	O (Wat2)	2.2	
	S (MCR)		2.4
	O2 (MCR)		2.6
Zn1	Zn2	3.5	3.6

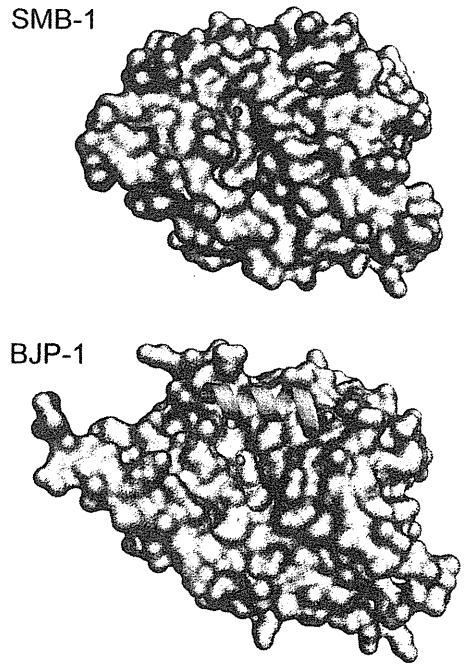

FIG 4 Molecular surface representations of SMB-1 and BJP-1. The N-terminal regions of SMB-1 and BJP-1 are shown as green and cyan secondary structures, respectively. The zinc ions in the active-site cavity are shown as spheres. The figures were drawn with PyMOL.

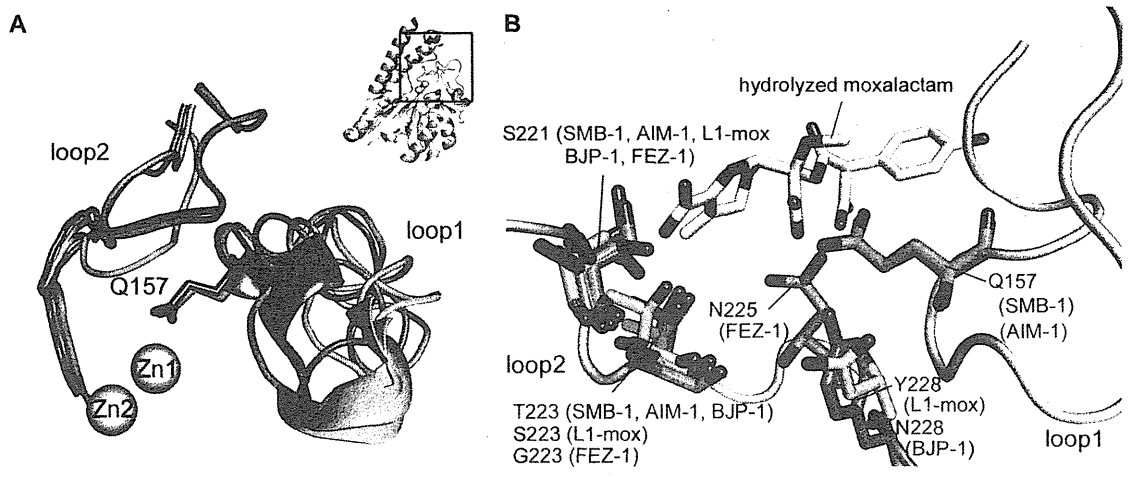

FIG 5 (A) Structural comparison of SMB-1 with AIM-1, L1, FEZ-1, and BJP-1, with particular focus on the two loop regions (loop1 and loop2). The overall structure of SMB-1 was drawn at right upper side. The part boxed with black lines in SMB-1 structure is enlarged and drawn with focus on the two loop regions. For SMB-1, the two loops are shown in green. The two zinc ions are shown as gray spheres. For AIM-1, L1, BJP-1, and FEZ-1, only the two loop regions are shown and are colored in slate blue, orange, cyan, and light pink, respectively. (B) Superposition of SMB-1 (green), AIM-1 (PDB code 4AWY; slate blue), L1-mox (PDB code 2AIO; orange), BJP-1 (PDB code 3LVZ, cyan), and FEZ-1 (PDB code 1K07, light pink) structures with focus on the residues, which are predicted to be involved in β-lactam recognition. The hydrolyzed moxalactam in the L1-mox structure is indicated with yellow sticks.

We hypothesized that various substrate preferences among the subclass B3 MBLs could be attributed to structural differences in the two loop regions. In fact, some of the amino acid residues in these two loop regions are already known to be responsible for binding to the substrate β-lactam antibiotics and/or inhibitor agents, as revealed by the complexed structures of BJP-1-4-nitrobenzenesulfonamide and L1-hydrolyzed moxalactam (34, 42) and also by site-directed mutagenesis approaches (41, 43).

In subclass B1 MBLs, the N233 residue was thought to play a role in β-lactam recognition, by facilitating creation of an oxyanion hole with the carbonyl oxygen of the β-lactam ring (44). In superposition of the SMB-1 structure with that of IMP-1, the tip of the Q157[113] residue in loop1 of SMB-1, whose amide side chain is located at 3.9 Å from Zn1, was positioned similarly to N233 of IMP-1. This suggests the possibility that the role of Q157[113] of SMB-1 corresponds to that of N233 of IMP-1. Q157[113] is a unique residue observed only in horizontally acquired subclass B3 MBLs, such as SMB-1 and AIM-1, but not in chromosomally encoded intrinsic subclass B3 MBLs, such as L1, BJP-1, and FEZ-1. Lerios et al. created an *in silico* docking model of an AIM-1-hydrolyzed cefoxitin structure and revealed the contacts between NE2 of Q157 and an oxygen of the C8 carboxylate group and also between NE2 of Q157 and a C10 carbonyl oxygen of hydrolyzed cefoxitin (20). Thus, the Q157[113] residue of SMB-1 would also contribute to the recognition of β-lactams, as it does in AIM-1. To elucidate the role of the Q157[113] residue in greater detail, we engineered a mutant in which the Q157[113] residue was replaced by an alanine; we established the steady-state kinetic constants of this molecule and tested its susceptibility. The Q157A[113] mutant protein showed increased K_m values for ampicillin, cefotaxime, ceftazidime, and imipenem, although the k_{cat} values for ampicillin and cefotaxime were somewhat increased (Table 3). In all, for the tested six β-lactams, the decrease in catalytic efficiency (k_{cat}/K_m) through alanine replacement at the Q157[113] residue was not large, which corresponded to the moderate reduction in MIC observed (Table 3). In the case of AIM-1, the replacement of residue 157 by alanine caused only a modest decrease in catalytic efficiency (k_{cat}/K_m) for a variety of β-lactams, which is consistent with the case of SMB-1 (20). Thus, Q157[113] is likely to be nonessential for hydrolytic activity of SMB-1 (also in AIM-1) but seems to play a role in enhanced hydrolytic activity for β-lactams compared to the other subclass B3 MBLs, probably by increasing the ability of enzyme to bind to substrate. Residues in other MBLs playing a role similar to that of Q157[113] in SMB-1 are postulated to be Y228 and N228 in L1 and BJP-1 and N225 in FEZ-1, but all of these are provided by the loop2 region (Fig. 5B).

TABLE 3 Kinetic parameters and result of susceptibility testing[a]

Substrate	β-Lactamase	K_m (μM)	k_{cat} (s^{-1})	k_{cat}/K_m ($M^{-1}\ s^{-1}$)	MIC (μg/ml)
Ampicillin	Wild	102	247	2.4×10^6	> 512
	Q157A	200	305	1.5×10^6	512
	Control	–	–	–	2
Ceftazidime	Wild	57	4.4	7.7×10^4	128
	Q157A	259	0.32	1.2×10^3	32
	Control	–	–	–	0.25
Cefotaxime	Wild	35	31	8.9×10^5	4
	Q157A	240	44	1.8×10^5	1
	Control	–	–	–	0.03
Cefepime	Wild	747	2.7	3.6×10^3	0.13
	Q157A	428	0.28	6.5×10^2	0.06
	Control	–	–	–	0.015
Imipenem	Wild	133	518	3.9×10^6	4
	Q157A	600	248	4.1×10^5	1
	Control	–	–	–	0.25
Meropenem	Wild	144	604	4.2×10^6	2
	Q157A	102	167	1.6×10^6	0.5
	Control	–	–	–	0.03

[a] The standard deviations for each parameter were below 20%. The data for the wild-type enzyme are from the reference 15. –, Not applicable.

In the structure of L1 with hydrolyzed moxalactam (PDB code 2AIO), interaction was observed between the S223 residue in loop2 and the C4 carboxylate group of hydrolyzed moxalactam (Fig. 5B). The T223[177] residue in SMB-1 was situated in the same position as the S223 residue in the L1 structure (Fig. 5B) and is likely to be involved in β-lactam substrate recognition. On the other hand, no such interaction was observed in the narrow-spectrum FEZ-1 due to the absence of a side chain at the G223 residue (Fig. 5B). The lower affinity of FEZ-1 for meropenem was also simulated in an *in silico* model by Liang et al. (45), which showed no such interactions, except for with the lactam motif. Although the main chain conformation surrounding the C4 carboxylate group differs little between subclass B3 MBLs, the slight difference in the position and orientation of side chains may influence the recognition of β-lactams.

Overall, it is likely that SMB-1 can accommodate a wider range of β-lactams by having more amino acid residues like Q157[113] around the active site, which are probably needed for recognition of the substrate β-lactams, than do BJP-1 and FEZ-1, subclass B3 MBLs with high K_m values for various β-lactams. This would explain the observed extended-spectrum activity of SMB-1 compared to BJP-1 and FEZ-1. Further structural analysis of SMB-1 in complex with various β-lactams would yield further insights into this proposal.

Binding mode of MCR in the active site. MCR is known as a reversible competitive inhibitor against the IMP-1 MBL, which belongs to subclass B1 (46). We determined the K_i value of SMB-1 for MCR to be 9.4 ± 0.4 μM, suggesting that MCR could behave as a potent inhibitor for SMB-1. Based on this finding, MCR was soaked into the SMB-1 crystal, and the complex structure was solved to 2.2 Å. In the SMB-1–MCR complexed structure, one MCR molecule was bound to the active site (Fig. 3B) to which β-lactams would originally bind. The thiolate group of MCR in the complexed structure replaced the bridging hydroxide anion (Wat1) between Zn1 and Zn2 observed in the native structure, where the thiolate group is bridged to two zinc ions (Zn1 and Zn2) with the distances of 2.2 Å for Zn1-S (MCR) and 2.4 Å for Zn2-S (MCR), respectively (Table 2). The Zn1-S (MCR) and Zn2-S (MCR) distances are close to those found in the D-captopril–L1 complex (2.3 and 2.2 Å) and the VIM-2–mercaptocarboxylate inhibitor complex (2.5 and 2.1 Å) (47, 48). Not only the thiolate group, but also the O2 atom of the carboxylate group in MCR is bound to Zn2 (2.6 Å), resulting in formation of a stable five-membered chelate ring (Fig. 3B); in most of the structures of MBLs complexed with compounds including a thiolate group determined thus far, only the thiolate group of the compound was coordinated to zinc ions (47–50).

In addition, the O2 atom of MCR forms a hydrogen bond to the hydroxyl OG of S221[175] (2.6 Å), and the O1 atom is involved in two hydrogen bonds with the hydroxyl OG1 of T223[177] (2.7 Å) and a water molecule (Wat3) (3.0 Å) (Fig. 3B). In the L1-hydrolyzed-moxalactam complexed structure (42), residues S221 and S223, which spatially correspond to S221[175] and T223[177] of SMB-1, were involved in the β-lactam recognition (Fig. 5B).

Furthermore, it is noteworthy that the binding of MCR to the active site causes a change in the coordination geometry of Zn2. The coordination around Zn1 in the complexed structure has a distorted tetrahedral geometry, which is similar to that in the native structure. On the other hand, the coordination around Zn2 in the complexed structure changed from a distorted square pyramid to a distorted trigonal bipyramid (Fig. 3B); the τ parameter was 0.83 {$\tau = [\beta-\alpha]/60$, where $\alpha = 120°$ for S (MCR)-Zn2-H263[215] NE2 and $\beta = 170°$ for O2 (MCR)-Zn2-D120[76] OD2}. Zn2 is located above 0.28 Å from the trigonal plane defined by H121[77] NE2, H263[215] NE2, and the thiolate group (S2) of MCR. The apical coordination sites are occupied by D120[76] OD2 and the carboxylate oxygen atom (O2) of MCR. The bond angle of O2 (MCR)-Zn2-D120[76] OD2 is 170° and the sum of the equatorial angles is 354°; 111° (H121[77] NE2-Zn2-H263[215] NE2), 123° (H121[77] NE2-Zn2-S2 (MCR)], and 120° (H263[215] NE2-Zn2-S2). The introduction of MCR yielded a slight increase (0.1 Å) in the distance between Zn1 and Zn2, compared to the native structure (Table 2). The structural observation of the binding mode of MCR to SMB-1 demonstrated that the mechanism of inhibition by MCR depended on the fact that the thiol group of MCR occupied the space, at which the hydroxide anion nucleophile (Wat1), which was assumed to contribute to the attacking on the carbonyl oxygen of the β-lactam ring, should originally locate.

Although a variety of the organic compounds, including a thiol group, have been designed and synthesized as MBL inhibitors, none have been used clinically (48, 51). Another possible use of these inhibitors is in development of a practical screening method for identification of MBL producers in the clinical microbiology setting (22, 23). The structure of the MCR complex presented here strongly suggests the potential and broad versatility of MCR as an MBL inhibitor. Thus, a screening approach employing MCR as an inhibitor would be universally applicable for identifying pathogenic bacteria that produce MBLs, including subclass B1 and B3 MBLs, as well as other MBLs that may emerge in future.

Conclusions. We report here the crystal structure of a subclass B3 MBL, SMB-1, and that of its complex with MCR. The higher catalytic efficiency against a wide range of β-lactams that was observed for SMB-1 could be attributed to the protein having a space capable of accommodating a wide range of β-lactams even with a bulky R1 side chain, provided by a loss of the long N terminus structure as observed in BJP-1, which includes residues such as F31 that prevent β-lactams from binding to the active site. Moreover, the presence of the amino acids such as Q157[113] provided by the loop regions would also contribute to recognition of β-lactams. Taken together, the difference in the accessibility of β-lactams to the active site and in the mode of β-lactam recognition by the residues from the two loop regions would influence the ability of the enzyme to recognize and catalyze β-lactams between subclass B3 MBLs, resulting in the major differences in the enzymatic behavior of subclass B3 MBLs.

In addition, through the inhibitor complexed structure, we could provide a rational model for the precise mode of inhibition of MCR on MBLs. MCR binds to the active site mainly by interaction with zinc ions, which is conserved in all of the MBLs found thus far. Therefore, a small MCR molecule would behave as a potent, universal inhibitor against MBLs, including subclass B1 and B3 MBLs. Moreover, MCR could be a powerful tool for screening for MBL-producing pathogenic bacteria in a clinical microbiology laboratory setting. Although commercially available serine–β-lactamase inhibitors, such as clavulanic acid, sulbactam, and tazobactam, are currently coadministered with antibiotic therapy, no MBL inhibitors have been marketed to date. The knowledge obtained from the structure presented here can shed

light on development of a potent inhibitor for MBLs, and may help in overcoming carbapenem resistance.

ACKNOWLEDGMENTS

This study was supported by grants from the Japanese Ministry of Education, Culture, Sports, Science, and Technology (Wakate B) and the Japanese Ministry of Health, Labor, and Welfare (H24-Shinkou-Ippan-010).

We are grateful to the staff of the Beamline BL-5A and NW12A at the Photon Factory (Tsukuba, Japan).

REFERENCES

1. **Nordmann P, Naas T, Poirel L.** 2011. Global spread of carbapenemase-producing *Enterobacteriaceae*. Emerg. Infect. Dis. 17:1791–1798.
2. **Galleni M, Lamotte-Brasseur J, Rossolini GM, Spencer J, Dideberg O, Frere JM.** 2001. Standard numbering scheme for class B β-lactamases. Antimicrob. Agents Chemother. 45:660–663.
3. **Walsh TR, Hall L, Assinder SJ, Nichols WW, Cartwright SJ, MacGowan AP, Bennett PM.** 1994. Sequence analysis of the L1 metallo-β-lactamase from *Xanthomonas maltophilia*. Biochim. Biophys. Acta 1218:199–201.
4. **Bellais S, Leotard S, Poirel L, Naas T, Nordmann P.** 1999. Molecular characterization of a carbapenem-hydrolyzing β-lactamase from *Chryseobacterium* (*Flavobacterium*) *indologenes*. FEMS Microbiol. Lett. 171:127–132.
5. **Saavedra MJ, Peixe L, Sousa JC, Henriques I, Alves A, Correia A.** 2003. Sfh-I, a subclass B2 metallo-β-lactamase from a *Serratia fonticola* environmental isolate. Antimicrob. Agents Chemother. 47:2330–2333.
6. **Rasmussen BA, Gluzman Y, Tally FP.** 1990. Cloning and sequencing of the class B β-lactamase gene (*ccrA*) from *Bacteroides fragilis* TAL3636. Antimicrob. Agents Chemother. 34:1590–1592.
7. **Docquier JD, Pantanella F, Giuliani F, Thaller MC, Amicosante G, Galleni M, Frere JM, Bush K, Rossolini GM.** 2002. CAU-1, a subclass B3 metallo-β-lactamase of low substrate affinity encoded by an ortholog present in the *Caulobacter crescentus* chromosome. Antimicrob. Agents Chemother. 46:1823–1830.
8. **Stoczko M, Frere JM, Rossolini GM, Docquier JD.** 2006. Postgenomic scan of metallo-β-lactamase homologues in rhizobacteria: identification and characterization of BJP-1, a subclass B3 ortholog from *Bradyrhizobium japonicum*. Antimicrob. Agents Chemother. 50:1973–1981.
9. **Osano E, Arakawa Y, Wacharotayankun R, Ohta M, Horii T, Ito H, Yoshimura F, Kato N.** 1994. Molecular characterization of an enterobacterial metallo β-lactamase found in a clinical isolate of *Serratia marcescens* that shows imipenem resistance. Antimicrob. Agents Chemother. 38:71–78.
10. **Lauretti L, Riccio ML, Mazzariol A, Cornaglia G, Amicosante G, Fontana R, Rossolini GM.** 1999. Cloning and characterization of bla_{VIM}, a new integron-borne metallo-β-lactamase gene from a *Pseudomonas aeruginosa* clinical isolate. Antimicrob. Agents Chemother. 43:1584–1590.
11. **Yong D, Toleman MA, Giske CG, Cho HS, Sundman K, Lee K, Walsh TR.** 2009. Characterization of a new metallo-β-lactamase gene, bla_{NDM-1}, and a novel erythromycin esterase gene carried on a unique genetic structure in *Klebsiella pneumoniae* sequence type 14 from India. Antimicrob. Agents Chemother. 53:5046–5054.
12. **Toleman MA, Simm AM, Murphy TA, Gales AC, Biedenbach DJ, Jones RN, Walsh TR.** 2002. Molecular characterization of SPM-1, a novel metallo-β-lactamase isolated in Latin America: report from the SENTRY antimicrobial surveillance programme. J. Antimicrob. Chemother. 50: 673–679.
13. **Castanheira M, Toleman MA, Jones RN, Schmidt FJ, Walsh TR.** 2004. Molecular characterization of a β-lactamase gene, bla_{GIM-1}, encoding a new subclass of metallo-β-lactamase. Antimicrob. Agents Chemother. 48: 4654–4661.
14. **Lee K, Yum JH, Yong D, Lee HM, Kim HD, Docquier JD, Rossolini GM, Chong Y.** 2005. Novel acquired metallo-β-lactamase gene, bla_{SIM-1}, in a class 1 integron from *Acinetobacter baumannii* clinical isolates from Korea. Antimicrob. Agents Chemother. 49:4485–4491.
15. **Wachino J, Yoshida H, Yamane K, Suzuki S, Matsui M, Yamagishi T, Tsutsui A, Konda T, Shibayama K, Arakawa Y.** 2011. SMB-1, a novel subclass B3 metallo-β-lactamase, associated with ISCR1 and a class 1 integron, from a carbapenem-resistant *Serratia marcescens* clinical isolate. Antimicrob. Agents Chemother. 55:5143–5149.
16. **Crowder MW, Walsh TR, Banovic L, Pettit M, Spencer J.** 1998. Overexpression, purification, and characterization of the cloned metallo-β-lactamase L1 from *Stenotrophomonas maltophilia*. Antimicrob. Agents Chemother. 42:921–926.
17. **Horsfall LE, Izougarhane Y, Lassaux P, Selevsek N, Lienard BM, Poirel L, Kupper MB, Hoffmann KM, Frere JM, Galleni M, Bebrone C.** 2011. Broad antibiotic resistance profile of the subclass B3 metallo-β-lactamase GOB-1, a di-zinc enzyme. FEBS. J. 278:1252–1263.
18. **Mercuri PS, Bouillenne F, Boschi L, Lamotte-Brasseur J, Amicosante G, Devreese B, van Beeumen J, Frere JM, Rossolini GM, Galleni M.** 2001. Biochemical characterization of the FEZ-1 metallo-β-lactamase of *Legionella gormanii* ATCC 33297T produced in *Escherichia coli*. Antimicrob. Agents Chemother. 45:1254–1262.
19. **Rossolini GM, Condemi MA, Pantanella F, Docquier JD, Amicosante G, Thaller MC.** 2001. Metallo-β-lactamase producers in environmental microbiota: new molecular class B enzyme in *Janthinobacterium lividum*. Antimicrob. Agents Chemother. 45:837–844.
20. **Leiros HK, Borra PS, Brandsdal BO, Edvardsen KS, Spencer J, Walsh TR, Samuelsen O.** 2012. Crystal structure of the mobile metallo-β-lactamase AIM-1 from *Pseudomonas aeruginosa*: insights into antibiotic binding and the role of Gln157. Antimicrob. Agents Chemother. 56:4341–4353.
21. **Toleman MA, Bennett PM, Walsh TR.** 2006. ISCR elements: novel gene-capturing systems of the 21st century? Microbiol. Mol. Biol. Rev. 70:296–316.
22. **Shibata N, Doi Y, Yamane K, Yagi T, Kurokawa H, Shibayama K, Kato H, Kai K, Arakawa Y.** 2003. PCR typing of genetic determinants for metallo-β-lactamases and integrases carried by gram-negative bacteria isolated in Japan, with focus on the class 3 integron. J. Clin. Microbiol. 41:5407–5413.
23. **Tsutsui A, Suzuki S, Yamane K, Matsui M, Konda T, Marui E, Takahashi K, Arakawa Y.** 2011. Genotypes and infection sites in an outbreak of multidrug-resistant *Pseudomonas aeruginosa*. J. Hosp. Infect. 78:317–322.
24. **Wachino J, Yamaguchi Y, Mori S, Yamagata Y, Arakawa Y, Shibayama K.** 2011. Crystallization and preliminary X-ray analysis of the subclass B3 metallo-β-lactamase SMB-1 that confers carbapenem resistance. Acta Crystallogr. Sect. F Struct. Biol. Crystallogr. Commun. 68:343–346.
25. **Otwinowski Z, Minor W.** 1997. Processing of X-ray diffraction data collected in oscillation mode. Methods Enzymol. 276:307–326.
26. **Vagin A, Teplyakov A.** 2010. Molecular replacement with MOLREP. Acta Crystallogr. D Biol. Crystallogr. 66:22–25.
27. **Dodson EJ, Winn M, Ralph A.** 1997. Collaborative Computational Project, number 4: providing programs for protein crystallography. Methods Enzymol. 277:620–633.
28. **Emsley P, Cowtan K.** 2004. Coot: model-building tools for molecular graphics. Acta Crystallogr. D Biol. Crystallogr. 60:2126–2132.
29. **Murshudov GN, Vagin AA, Dodson EJ.** 1997. Refinement of macromolecular structures by the maximum-likelihood method. Acta Crystallogr. D Biol. Crystallogr. 53:240–255.
30. **Lovell SC, Davis IW, Arendall WB III, de Bakker PI, Word JM, Prisant MG, Richardson JS, Richardson DC.** 2003. Structure validation by Cα geometry: ϕ,ψ and Cβ deviation. Proteins 50:437–450.
31. **Clinical and Laboratory Standards Institute.** 2009. Methods for dilution antimicrobial susceptibility tests for bacteria that grow aerobically. Approved standard, 8th ed. Document M07-A8. CLSI, Wayne, PA.
32. **Garau G, Garcia-Saez I, Bebrone C, Anne C, Mercuri P, Galleni M, Frere JM, Dideberg O.** 2004. Update of the standard numbering scheme for class B β-lactamases. Antimicrob. Agents Chemother. 48:2347–2349.
33. **Carfi A, Pares S, Duee E, Galleni M, Duez C, Frere JM, Dideberg O.** 1995. The 3-D structure of a zinc metallo-β-lactamase from *Bacillus cereus* reveals a new type of protein fold. EMBO J. 14:4914–4921.
34. **Docquier JD, Benvenuti M, Calderone V, Stoczko M, Menciassi N, Rossolini GM, Mangani S.** 2010. High-resolution crystal structure of the subclass B3 metallo-β-lactamase BJP-1: rational basis for substrate specificity and interaction with sulfonamides. Antimicrob. Agents Chemother. 54:4343–4351.
35. **Garcia-Saez I, Mercuri PS, Papamicael C, Kahn R, Frere JM, Galleni M, Rossolini GM, Dideberg O.** 2003. Three-dimensional structure of FEZ-1, a monomeric subclass B3 metallo-β-lactamase from *Fluoribacter gormanii*, in native form and in complex with D-captopril. J. Mol. Biol. 325:651–660.
36. **Ullah JH, Walsh TR, Taylor IA, Emery DC, Verma CS, Gamblin SJ, Spencer J.** 1998. The crystal structure of the L1 metallo-β-lactamase from